THE ULTRASTRUCTURE OF MAUTHNER CELL SYNAPSES AND NODES IN GOLDFISH BRAINS

J. DAVID ROBERTSON, M.D., THOMAS S. BODENHEIMER, and DAVID E. STAGE

From the Department of Neurology and Psychiatry, Harvard Medical School, Boston, and the Research Laboratory, McLean Hospital, Belmont, Massachusetts

ABSTRACT

An electron microscope study of goldfish Mauthner cells is reported.[1] The cell is covered by a synaptic bed $\sim 5\ \mu$ thick containing unusual amounts of extracellular matrix material in which synapses and clear glia processes are implanted. The preterminal synaptic neurites are closely invested by an interwoven layer of filament-containing satellite cell processes. The axoplasm of the club endings contains oriented mitochondria, neurofilaments, neurotubules, and relatively few synaptic vesicles. That of the boutons terminaux contains many unoriented mitochondria and is packed with synaptic vesicles and some glycogen but no neurofilaments or neurotubules. The bare axons of club endings are surrounded by a moderately abundant layer of matrix material. The synaptic membrane complex (SMC) in cross-section shows segments of closure of the synaptic cleft ~ 0.2 to $0.5\ \mu$ long. These alternate with desmosome-like regions of about the same length in which the gap widens to ~ 150 A and contains a condensed central stratum of dense material. Here, there are also accumulations of dense material in pre- and postsynaptic neuroplasm. The boutons show no such differentiation and the extracellular matrix is largely excluded around them. The axon cap is a dense neuropil of interwoven neural and glial elements free of myelin. It is covered by a closely packed layer of glia cells. The findings are interpreted as suggestive of electrical transmission in the club endings.

INTRODUCTION

Teleost brains contain two nerve cells which are of an unusually large size for vertebrates. They measure from 0.5 mm to over 1 mm in length by as much as 60 μ in diameter. These giant cells bear the name of Mauthner who, in 1859 (77), discovered their giant axons in fish spinal cords. They have been studied extensively with the light microscope by Beccari (7) in 1908, Bartelmez (5) in 1915, Bartelmez and Hoerr (6) in 1933, and more recently by Bodian (11–13) and others (17, 92, 94, 95). This paper reports the first results of an investigation of these cells and their synapses by electron microscopy.[2] A new type of vertebrate synaptic contact has been found, and a surprisingly

[1] The work presented has been reported in abstract form (119).

[2] McGee-Russell and Palay (80) have taken some unpublished electron micrographs of the club endings of Mauthner cells that became known to us after our work was completed.

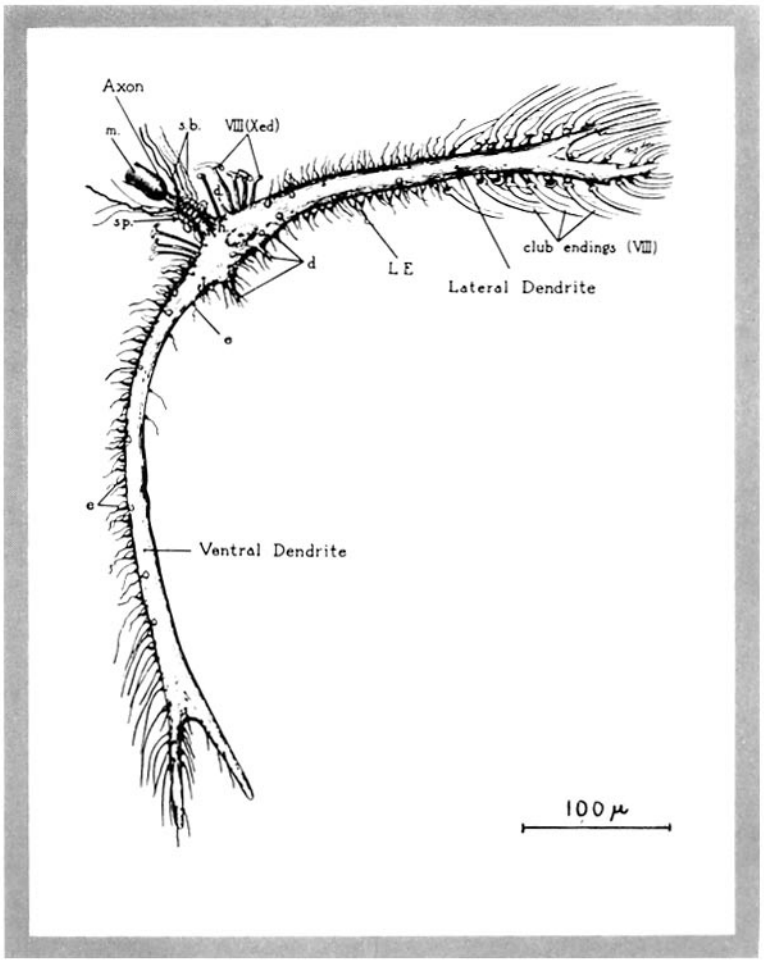

The magnification markers represent 1 μ unless otherwise stated.

FIGURE 1 Diagram taken with labels taken from Bodian (1) showing a Mauthner cell with its various synapses. *d*, small dendrites; *e*, small end bulbs; *h*, axon hillock; LE, large end bulbs; *m*, myelin sheath of Mauthner axon; sb, bundle giving origin to spiral fibers; sp, spiral fibers in region of "axon cap"; VIII (Xed), crossed vestibular fibers giving rise to collaterals which terminate as small club endings; and VIII, vestibular root fibers.

abundant extracellular matrix material, not hitherto recognized in vertebrate central nervous systems (CNS), has been identified about synapses and at nodes.

The giant Mauthner cells are found in teleosts; they are also found in frog tadpoles but regress after metamorphosis (126). Fig. 1 is a diagram taken from Bodian (11) that summarizes the general features of the cells in goldfish as seen by light microscopy. The nucleus of each of the cells in goldfish 3 to 4 inches long is located ~1 mm above the ventral surface of the medulla ~0.3 mm lateral to the midline just cranial to the level of the entrance of the eighth nerves. The cell is peculiar in having, besides the usual smaller dendrites, a very large so called lateral dendrite running in a latero-caudal direction and a slightly smaller so called ventral dendrite running in a ventro-cranial direction. The axon runs dorsomedially from the nuclear region. It decussates with the opposite Mauthner axon at the midline just beneath the floor of the 4th ventricle and turns caudally to run into the spinal cord, giving off branches to motor horn cells at various levels.

The first 40 to 50 μ of the axon narrows to $\sim$10 μ in diameter and is unmyelinated. It is surrounded by a specialized neuropil $\sim$80 to 90 μ in diameter called the axon cap. Upon leaving the cap the axon expands rapidly to a diameter of $\sim$30 to 35 μ and becomes heavily myelinated.

The reader may very roughly visualize a Mauthner cell in the medulla in the following way. Hold one hand before the eyes with the fingers fully extended and arm outstretched. Imagine a line of sight running cranially along the longitudinal axis of the medulla from the eye through the hand. Let the dorsal direction be upwards. Point the forefinger toward the opposite shoulder and the thumb downwards and slightly away from the body. The forefinger represents the lateral dendrite and the thumb the ventral dendrite with the nucleus between the bases of the thumb and forefinger. The axon roughly follows the line of the arm. If both hands are placed in position at the same time the crossing of the wrists represents the decussation of the axons.

The entire Mauthner soma dendrite, except for the lateral surface of the ventral dendrite, is covered by numerous synapses. The axon hillock is surrounded by a dense, roughly spherical, neuropil consisting of intermingled neural and glial fibers. It contains some fairly large axons that appear to be wrapped spirally around the Mauthner axon. The whole neuropil is bordered by a layer of special glia cells. This axon hillock apparatus is referred to as the "axon cap." The lateral part of the lateral dendrite shows numerous so called club endings. These are blunt perpendicular terminations of fairly large myelinated fibers against the lateral dendrite. They lose their myelin sheath abruptly at the ending and the axon simply flattens out over the dendrite surface with a very slight increase in its diameter. The other major endings are boutons terminaux. These are characterized by a sudden bulb-like expansion of a very small neurite to several times its diameter as it spreads out over the postsynaptic membrane. We have experienced no difficulty in identifying the club endings with the electron microscope and the boutons have posed no great problem since the characteristics in electron micrographs of this general kind of ending have been described by Palay (85) and others. We feel confident, therefore, that we have correctly identified these two general types of endings with the ones previously described by light microscopy.

The large club endings on the lateral dendrites are known to be VIIIth nerve endings (5, 6, 11). Some small club endings occurring on the cell body near the nucleus are stated to be VIIIth nerve fibers crossed over from the other side (13). The origins of the boutons are less precisely known.

By virtue of large size and a thick myelin sheath the Mauthner axons have conduction velocities that are much higher than those of any other nerve fibers in the spinal cord. Bartelmez (5) states that they are part of a three cell reflex arc with the main sensory input coming in from the VIIIth nerve endings on the lateral dendrite and efferent impulses leaving from motor horn cells in the spinal cord. More recently, however, Wilson (134) has produced electrophysiological evidence indicating that vestibular stimulation by displacement, tilting, or acceleration is alone not enough to fire off the Mauthner axons in *Protopterus* (lungfish). By microelectrode recordings from Mauthner axons it was shown that a sharp single spike was obtained only as a startle response elicited by a severe jar to the aquarium. This is followed by a sudden flip of the tail. The ratio of input stimuli to output was very high and it appeared that only a special combination of stimuli would elicit a response. It seems then that the Mauthner cell system functions as an escape mechanism. In this sense it may be analogous to the giant fiber synapse systems of crayfish, prawns, etc. It is clear that very fast, sure fire synaptic transmission is needed in any such system. We have found evidence of a structural specialization in the club synapses that, to us, is suggestive of electrical transmission, a feature that may be directly related to this need.

MATERIALS AND METHODS

Common goldfish (*Carassius auratus*) obtained from Grassyfork Fisheries in Saddle River, New Jersey, ranging from 2 to 4 inches in length, were used throughout. The fish were kept in a conventional aquarium in recirculated tap water freed of chlorine and filtered through charcoal and a gravel bottom filter.

The brains were fixed in several different ways with variations of the perfusion technique of Palay *et al.* (86). The most informative specimens were fixed by a combination formalin–OsO_4 method according to Pease (88), using formalin made up especially according to Richardson's method (97). All of the preparations were embedded in Araldite by a modification of the method of Glauert, Rogers, and Glauert (46), and most were stained with saturated uranyl acetate (132) or permanganate (66). The modifica-

TABLE I

Solution	Component	gm/liter
1. Goldfish Ringer*	NaCl	5.85
	KCl	0.19
	$CaCl_2$	0.17
	$NaHCO_3$	0.42
	$MgCl_2 \cdot 6H_2O$	2.03
	$NaH_2PO_4 \cdot H_2O$	0.07
2. Formalin Fixative‡		
	A. $NaH_2PO_4 \cdot H_2O$	22.6
	B. NaOH	25.2
	C.§ Paraformaldehyde (trioxymethylene; Matheson, Coleman, and Bell, East Rutherford, New Jersey)	400.0
	C.§ Glucose	54.0
	D. 41.5 ml solution A	
	D. 8.5 ml solution B	
	Fixative: 45.0 ml solution D	
	Fixative: 5.0 ml solution C	
3. OsO_4 Fixatives		
i. Standard (pH 7.4)	NaCl	4.71
	KCl	0.19
	$CaCl_2$	0.17
	$NaHCO_3$	0.42
	$MgCl_2 \cdot 6H_2O$	2.03
	$NaH_2PO_4 \cdot H_2O$	0.07
	OsO_4	10.0
ii. After Millonig (82)		
	A. 2.26 per cent $NaH_2PO_4 \cdot H_2O$	22.6
	B. 2.52 per cent NaOH	25.2
	C. 5.4 per cent Glucose	54.0
	D. 41.5 ml solution A	
	8.5 ml solution B	
	Fixative: 45.0 ml solution D	
	5.0 ml solution C	
	0.5 gm solid OsO_4	
iii. 2.5 per cent OsO_4	NaCl	2.98
	KCl	0.19
	$CaCl_2$	0.17
	$NaHCO_3$	0.42
	$MgCl_2 \cdot 6H_2O$	2.03
	$NaH_2PO_4 \cdot H_2O$	0.07
	OsO_4	25.0
4. Pal's Bleach (67)	$K_2SO_3 \cdot 2H_2O$ (potassium sulfite)	5.0
	$C_2O_4H_2 \cdot 2H_2O$ (oxalic acid)	5.0
5. Araldite (46)	Resin M, 50 ml	
	Hardener, 50 ml	
	Dibutylphthalate, 2.5 ml	
	Accelerator 964C, 1.5 ml	

* This solution was modified from one used by Forster and Taggart (36) by increasing the magnesium chloride content.

‡ The pH of all fixatives was adjusted to 7.4 to 7.6 by addition of a few drops of N HCl.

§ Methanol-free formalin (solution C) is prepared by dissolving 40 gm of paraformaldehyde powder in 100 ml of double distilled H_2O. The mixture is heated to 60 to 65°C and a few drops of 40 per cent NaOH are added until the solution becomes clear. 5.4 gm of glucose is then added.

tions of the embedding and staining techniques employed have been in use for several years but have not been published.[3] Since we have had consistently good results with these methods they will be described in some detail. The composition of the solutions used in all our procedures is given in Table I.

The technique for perfusing the brains was as follows: The fish were anesthetized by placing them in a beaker of 0.025 per cent tricaine methanesulfonate (Sandoz Pharmaceuticals, Hanover, New Jersey) in tap water until swimming movements ceased. The heart was exposed and 0.25 ml of Panheprin (Abbott Laboratories, North Chicago; 10,000 units/ml) was injected into the ventricle through a No. 27 needle. This was followed by 0.5 ml of a 0.7 per cent solution of sodium nitrite. The conus arteriosus was then opened and a polyethylene tube (Clay-Adams, Inc., New York, Intramedic PE 10 or PE 50, depending on the size of the fish) tied into the aorta. About 5 ml of Ringer solution at room temperature was then injected with a syringe at a moderate rate, flushing out most of the blood from the gills.The tube was then connected, taking care to eliminate bubbles, to a glass adaptor fed with fixative by a gravity drip perfusion apparatus at a 5 foot head of pressure.

In the case of formalin–OsO_4 fixation the first 10 ml (approximate) of the formalin fixative was at room temperature but the remainder was prechilled and passed through an ice-salt-water jacket about 10 inches long about 10 inches from the animal. The temperature of the fixative upon entering the animal was between 0° and 5°C. The fixative was allowed to flow at a rate of 5 to 10 ml/minute. After about 75 to 100 ml of the fixative was used it was replaced by Ringer (solution 1) to flush out excess formalin. After about 100 ml of the Ringer solution entered the animal it was replaced by one of the OsO_4 fixatives. After ~75 to 100 ml of the second fixative was used the brain was removed and placed directly into the OsO_4 fixative at ice water temperature. The total fixation time (both fixatives) was usually 4 hours. Sometimes the whole brain was left in the fixative for the full time and sometimes the medulla was cut, immediately upon removal to the fixative, into transverse slices 0.5 to 1.0 mm thick. There seemed little difference between these two procedures, the quality of the preparation apparently being determined by the uniformity of initial perfusion. If not already sliced, the medulla was finally sliced in 25 per cent acetone during dehydration. Each slice was numbered and placed in a Minicube polyethylene ice cube tray compartment of 2 ml capacity. Dehydration was carried out by replacing the volume of each compartment successively, using a glass pipette vacuum aspirator, by 25 per cent, 50 per cent, 75 per cent and three changes of 100 per cent acetone at time intervals of 10 minutes or more. The acetone was kept at 0 to 4°C until the final change, after which it was allowed to come slowly to room temperature. An additional change was then made at room temperature. The slice was then oriented with its caudal face down and the acetone aspirated thoroughly from the compartment. While still wet with acetone the specimen was covered carefully with Araldite (solution 5) and the ice cube tray placed *uncovered* in a dry oven at 60°C for 24 to 48 hours. This procedure almost always yields blocks of excellent cutting quality. The residual acetone evaporates in the oven and is replaced directly by Araldite of the correct composition for polymerization. This simple method avoids much of the difficulty experienced with the older Araldite techniques. The blocks readily separate from the ice cube tray.

A special hand microtome (to be described separately) was constructed to permit successive sections to be made free hand, with a razor blade, from the block faces to locate the Mauthner cell. The blocks were then trimmed to include only the desired area of the cell, and thin sections were cut with a Dupont diamond knife on an LKB microtome. The sections were lifted on carbon films and stained with saturated uranyl acetate at pH 5.4 or more frequently with 1.2 per cent $KMnO_4$ by a modification of the technique of Lawn (66). Since this modification has not been published, the technique will be described. About 2 ml of $KMnO_4$ is freshly withdrawn from below the surface of a stock bottle and placed in a tightly covered ~50 mm disposable plastic petri dish. The grids are floated, section down, on the $KMnO_4$ and the dish tightly covered. After about 30 minutes the grids are washed thoroughly with a jet of double distilled water and floated for 30 seconds on a freshly made 1:100 dilution of Pal's bleach (67) (solution 4). They are then rewashed and dried. Quite clean, well stained specimens can be regularly obtained with this technique.

The specimens were all examined with a Siemens Elmiskop 1b electron microscope under instrumental conditions given separately (118). Light microscopy was done with a Zeiss Ultraphot using phase contrast optics. Sections 0.6 to 1.6 μ thick were cut with a diamond knife, flattened with toluene vapor (122), transferred to a drop of water on a glass slide, blotted dry, and placed in 1.2 per cent $KMnO_4$ in a covered coplin jar for about 30 minutes. The slide was then dipped rapidly into distilled water, passed quickly through 1:10 Pal's solution and left in 1:100 Pal's solution for 60 seconds. It was then rinsed, dried,

[3] Some of the techniques were developed while the author was in charge of the electron microscopy laboratory in the Department of Anatomy at University College in London, England. Various aspects of the techniques of embedding and permanganate staining were suggested by Dr. Ruth Bellairs and Dr. Michael Kidd. Mrs. Rose Wheeler also gave valuable technical assistance in developing the methods.

TABLE II

Level of section	Lateral dendrite A	Lateral dendrite P	Lateral dendrite B
μ	μ	μ	μ
0	38	18	26
15	40	19	26
30	40	23	30
45	40	24	25
60	37	22	23
75	42	25	26
90	40	31	33

	Soma: Axis ∥ to axon A	Soma: Axis ∥ to axon P	Soma: Axis ∥ to axon B	Soma: Axis ⊥ to axon A	Soma: Axis ⊥ to axon P	Soma: Axis ⊥ to axon B	Axon cap A	Axon cap P	Axon cap B	Axon: Unmyelinated A	Axon: Unmyelinated P	Axon: Unmyelinated B	Axon: Myelinated A	Axon: Myelinated P	Axon: Myelinated B
μ		μ	μ	μ	μ	μ	μ	μ	μ	μ	μ	μ	μ	μ	μ
120	59			57			84						37		
125	62			60			83								
126	59	41	59	57	60	79	90						36		
127		Axon		54			86	74	43	9	7	7	31	27	29
128		adjoining		56			86			10			32		
130		cell		55			92						26	tangential	
132				55			88						24		
135	47			54			88								
140	37	28	36	51	62	67	74								
145	34			51			72								
150	33			50			57								
155	30	16	29	51	54	60	37								

Level of section	Ventral dendrite A	Ventral dendrite P	Ventral dendrite B
μ	μ	μ	μ
160	30		
175	33		
190	27	15	23
205	27		
208	30	16	23
220	33	17	20
250	34	18	23
265	40	17	24

covered with immersion oil under a coverslip, and examined. A longer staining time was used for Fig. 4.

In addition to using the techniques of electron microscopy, we have studied the Mauthner cell by various light microscope techniques including conventional paraffin-embedded sections of brains fixed and stained in various ways to provide background information for our electron microscope studies. The most informative material has been prepared by Davenport's modification of the Bodian protargol method (60).

RESULTS

Light Microscopy

A. General

We have studied extensively Mauthner cells prepared for electron microscopy but sectioned at about 1 μ thickness for study by phase contrast light microscopy. In one instance, after fixation with 2.5 per cent OsO_4 we cut sections serially through an entire Mauthner cell beginning with the lateral dendrite and ending with the terminal portion of the ventral dendrite. This cell was from a goldfish about 3 inches long. In this instance we examined sections at roughly 15 μ intervals until the axon cap was reached. Here we took samples at $\sim$5 μ intervals until the cap was passed, resuming the $\sim$15 μ steps thereafter. Thin sections for electron microscopy were cut adjacent to many of the sample sections for light microscopy.

Figs. 2 and 3 and 5 to 7 are sections of this Mauthner cell. The plane of sectioning included the axon in the axon cap in Fig. 6. This series covered a depth of $\sim$295 μ parallel to the longitudinal axis of the medulla. Since the Mauthner cell is oriented with the lateral dendrite running caudo-laterally and the ventral dendrite craniomedially it is difficult to measure its length directly. However, we were able to measure the diameters of the various parts of the cell with enough accuracy to provide useful figures and from a simple calculation get some idea of its length. The dimensions at various levels are given in Table II in column A. Zero designates the start of the series in the lateral dendrite. We estimated that at this point the dendrite lay roughly 635 μ lateral and 150 μ caudal to the nucleus. At the end of the series the end of the ventral dendrite lay about 565 μ ventral and 100 μ cranial to the nucleus. These figures permit us to make a very rough trigonometric calculation of the length of this particular cell. We calculate that it is $\sim$1.2 mm long.

The successive levels in the series of sections are designated as plus some number of microns in the cranial direction. The measurements were made along the minimum diameters of the dendrites to reduce the error imposed by the obliquity of the sectioning planes. In the nuclear regions the measurements were made as maximum dimensions along an axis parallel to the longitudinal axis of the axon and one perpendicular to this direction. In the axon hillock region the parallel measurements were omitted and the maximum diameter of the axon cap perpendicular to the longitudinal axis of the axon was recorded. The outer borders of the cap cells were taken as the boundary (large block arrows in Fig. 2). Some comparable measurements were made at about the same levels in sections of paraffin embedded material fixed in the one case with paratoluenesulfonic acid (PTSA) (72) (Table II, column P) and stained with hematoxylin and eosin, and in the other with formalin followed by staining with Davenport's modification of Bodian's protargol stain (60) (Table II, column B). These figures are included to give some rough idea of the comparable dimensions of the structures after embedding for electron microscopy as compared with ones embedded in paraffin. The dimensions are considerably smaller in the latter, except, curiously, for the cell body, but no effort was made to do a statistical study of these differences.

From the figures for the Araldite-embedded specimens we have made a rough estimate of the total volume of the cell. If the lateral dendrite is assumed to be a cylinder with a length of 650 μ and an average diameter of 40 μ, its volume would be $8.2 \times 10^5\ \mu^3$. If the cell body is taken to have a diameter of 56 μ, its volume is $9.2 \times 10^4\ \mu^3$. Similarly the volume of the ventral dendrite is about $4.6 \times 10^5\ \mu^3$. The total volume of the cell is, therefore, $\sim 10^6\ \mu^3$.

The particular series of Araldite embedded specimens did not include the terminal regions of the lateral and ventral dendrites but in other series we have noted that there are usually two main bifurcations of both the lateral and ventral dendrites at their ends, as pictured by Bodian. Further, we too have noted that there are occasional relatively small dendritic branches, particularly in the nuclear region. These sometimes enter the cap neuropil as in Fig. 6, again con-

firming the previous workers. Bartelmez (5) states that there are usually eight such dendrites in catfish.

Fig. 2 shows the nucleus and axon cap of the Mauthner cell measured in Table I. Note the folded nuclear membrane and the very prominent nucleolus. The nucleus measures about 30 μ in its smallest diameter and the nucleolus is about 5 to 6 μ in diameter. The cytoplasm shows numerous dense granules about 1 μ or less in diameter.

B. The Synaptic Bed

The entire surface of the Mauthner cell including the lateral and ventral dendrites, except for the lateral surface of the ventral dendrite, is covered by a zone about 5 μ thick that is clearly differentiated from the surrounding tissue (small block arrows in Fig. 2). This zone is generally free of myelin and contains many synaptic endings. We refer to it as the "synaptic bed." The club endings are easily identified in the synaptic bed. They are particularly prominent and large over the lateral dendrites (Fig. 3) but smaller ones occur elsewhere (Fig. 2, *C*). They are recognized by the presence of a myelin sheath that extends right into the synaptic bed and terminates only a few microns from the Mauthner cell surface and by the fact that the unmyelinated axon does not expand appreciably at the endings. Often they are of relatively large size, and striations are seen perpendicular to the synaptic membrane. The boutons terminaux are less easily identified by light microscopy. Sometimes, however, we have been able to make out their characteristics. They appear as granular bulb-like terminations of very small ($\sim$1 μ or less) fibers that enlarge abruptly to several microns in diameter spreading out over the Mauthner cell surface to assume a shape rather like that taken by a sealed plastic bag partially filled with water and set on a table top (Fig. 1). The connections between these endings and their parent neurites are usually not seen in our thin ($\sim$1 to 2 μ) sections.

The axon cap is easily identified as a roughly spherical rather dense neuropil enveloping the initial segment of the axon and the axon hillock region. It is free of myelin and this feature alone is sufficient to differentiate it from the surrounding tissue in which myelinated fibers dominate. A further differentiating feature is the distinct layer of glial cap cells whose nuclei are confined to the superficial boundary zone. The particular axon cap (*ax c* and large block arrows) in Fig. 2 is shown in different planes of sectioning in Figs. 5 and 6, and a different one including a part of the Mauthner axon is shown in Fig. 4 at higher magnification. In Fig. 4, the Mauthner axon (*M ax*) lies to the right. Note the polygonal cap cells (*c*) to the upper center. These form a compact pavement layer at the periphery of the cap and extend long tenuous processes down into the cap neuropil. Fig. 5 is a section tangent to the cap through this layer. The shapes of the cells are polygonal in this plane of sectioning as well as the one in Fig. 4, and the nuclei are more round.

Numerous small myelinated axons enter the cap by penetrating between the cap cells while losing their myelin. Branches of these axons may be recognized deep in the cap and we have followed some of them in a few serial sections by light microscopy. While we have not yet attempted any definitive serial section reconstructions, our findings suggest that they follow a spiral course around the axon and they may, therefore, be components of the spiral apparatus in the cap pictured by Bartelmez (5) and Bodian (11, 13).

FIGURE 2 Phase contrast light micrograph of $\sim$1 μ section near the axon hillock of a Mauthner cell. It shows the nucleus with its prominent nucleolus, the axon cap (*ax c* between apposed large block arrows to the right) and a part of the expanded myelinated Mauthner axon (*M ax*). The aligned block arrows to the left mark the synaptic bed. Note the small club ending at arrow *C*. 2.5 per cent OsO_4 fixation; $KMnO_4$ stain. Marker is 10 μ. $\times$ 900.

FIGURE 3 Phase contrast light micrograph of section of a lateral dendrite showing the synaptic bed (block arrows) and several club endings (thin arrows). 2.5 per cent OsO_4 fixation; $KMnO_4$ stain. Marker is 10 μ. $\times$ 900.

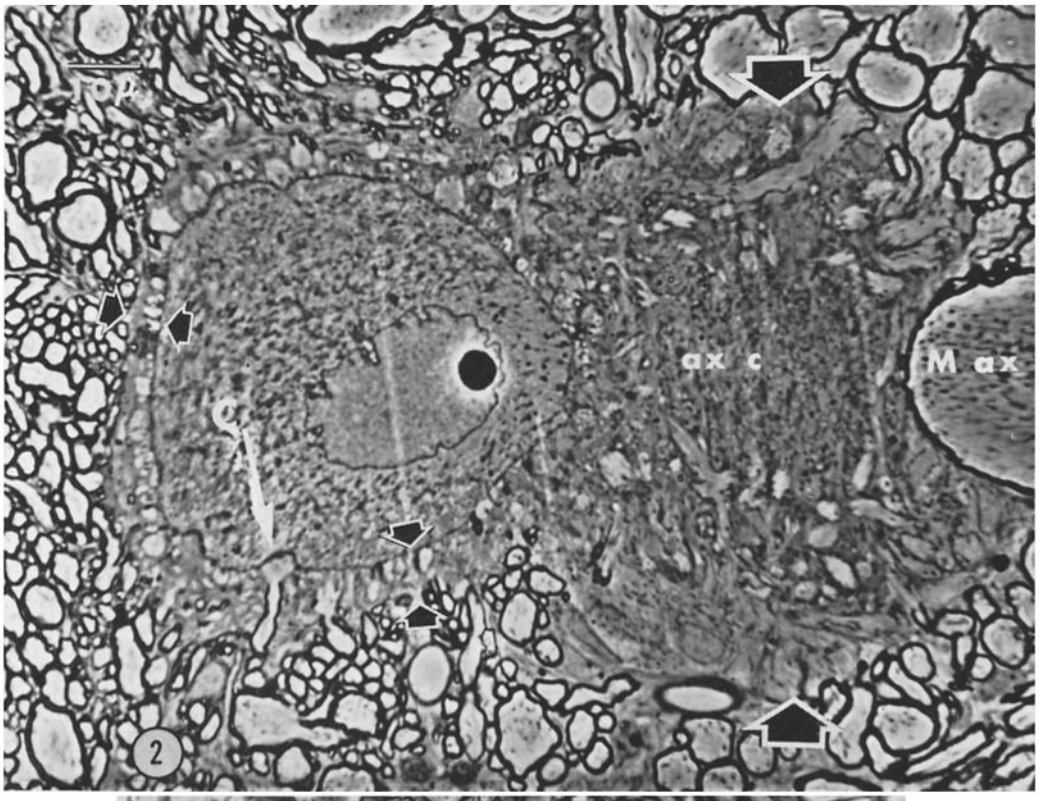
ax c
M ax
2

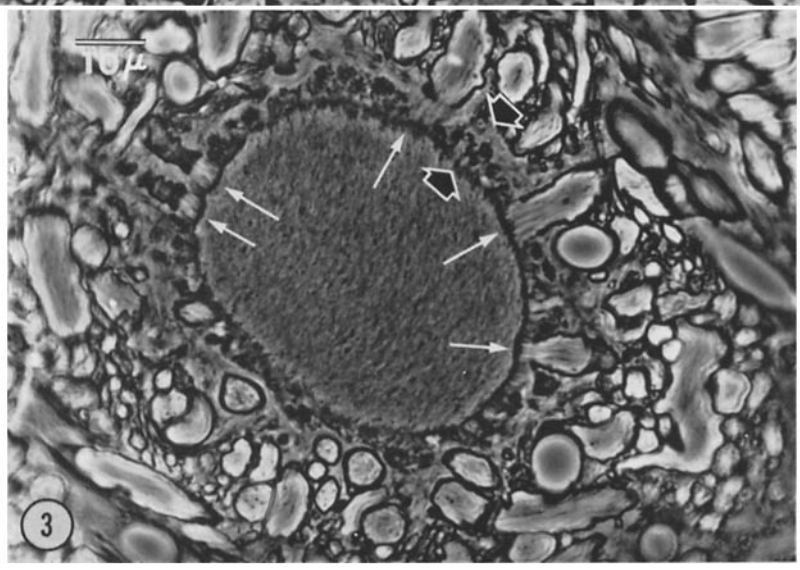
3

Electron Microscopy

A. General

Figs. 8 to 10 show myelinated fibers in the medulla well removed from the Mauthner cell. They are included partly to illustrate the general quality of fixation achieved but they also make certain points that are not clearly established in the literature. The presence of relatively large numbers of ~200 A neurotubules in dendrites, as demonstrated by Gray (48) in pyramidal cell dendrites, led at first to some tendency to use the presence of appreciable numbers of such tubular forms in a neurite profile as one of the criteria for identifying dendrites. That the problem is more complicated than this has been recognized more recently, and Wolfe (135) has given more detailed criteria in which he recognizes that the tubular forms also occur in axons. Our micrographs support this and show that the tubular forms may sometimes be quite abundant in axons (Fig. 8, left insets). In addition, assessment of their relative abundance is complicated by the fact that the relative number of tubular forms rises as the fiber diameter decreases (lower right inset, Fig. 8).

Similar tubular forms are generally also seen in the Mauthner cell. They may be seen prominently in longitudinal profile in the Mauthner lateral dendrite in Figs. 11, 12, 15, 25, and 30. They occur in the cell body at the nuclear level and are also found in the Mauthner axon (Figs. 35 and 36). Tubular forms occur in the axons of club endings (Fig. 30, lower inset, and Figs. 31–33). Perhaps statistical studies of their relative abundance in axons and dendrites will allow their relative numbers to be used as a guide, but, without such, caution should be exercised in using their presence even in dominant numbers as a criterion to identify dendrites except in combination with other more definite features.

Fig. 9 shows a group of myelinated fibers packed closely together so that in places their myelin sheaths become continuous by contact of the outside surfaces of the outermost unit membranes to make an extra intraperiod line (upper inset of area indicated by arrow *1*). This configuration was seen and interpreted in this way by Maturana (76) and Peters (89, 90). The regions marked *e* in the lower inset are bounded by the outside surfaces of unit membranes and hence are extracellular. The unit membrane strata do not show up clearly but the presence of the outer ones may be detected in the lower inset by the formation of an intraperiod line of myelin. However, since these spaces appear almost empty they could represent artifact.

Fig. 10 illustrates a neurite filled with vesicles in very close association with a myelinated fiber on one side and several relatively clear cellular profiles on the others. To the upper center (arrow *1* and upper inset enlargement) there is a desmosome-like region (~300 A across) in which the gap between the apposed membranes is widened and contains dense material. To either side but more marked below there is a slight accumulation of dense material in the cytoplasm next to the membranes. To the lower left (arrow *2* and lower inset) there is a region of contact between two membranes of clear cell profiles in

---

FIGURE 4 Higher magnification light micrograph of part of axon cap showing the Mauthner axon (*M ax*) to the right and several cap cells (*c*). Note the small myelinated axons (*ax*) entering between the cap cells and losing their myelin (compare with Fig. 33). Two capillaries (*cap*) are shown. Formalin–OsO_4 fixation; $KMnO_4$ stain. × 1500.

FIGURE 5 Tangential section of edge of axon cap showing several cap cells (*c*). 2.5 per cent OsO_4 fixation; $KMnO_4$ stain. × 1600.

FIGURE 6 Section of Mauthner cell in axon hillock region showing the axon cap (block arrows) and including the unmyelinated axon. Note the dendrite, (*d*), (inset), penetrating the cap neuropil. 2.5 per cent OsO_4-fixed; $KMnO_4$-stained. × 650; inset, × 1800.

FIGURE 7 Section of ventral dendrite. The medial surface is to the left. Note the synaptic bed (block arrows) here and its absence on the lateral surface. 2.5 per cent OsO_4-fixed; $KMnO_4$-stained. × 1000.

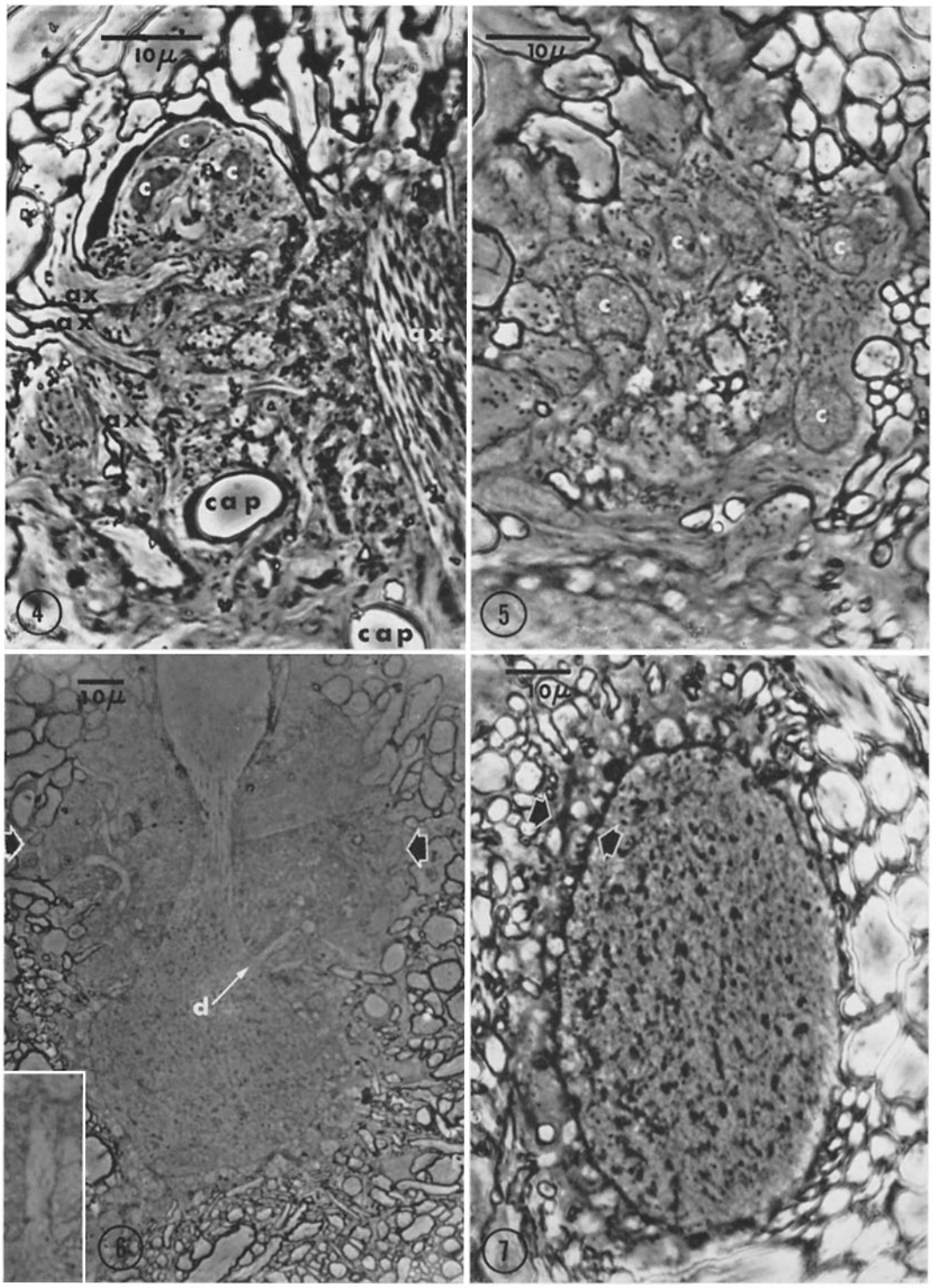
10μ
c
ax
cap
4
10μ
c
5
10μ
d
6
10μ
7

which the intervening gap is closed, making an external compound membrane measuring about 160 A across. A faint suggestion of the united outer strata of the unit membranes can be seen here in the inset enlargement to the lower left. This type of contact is like the ones previously described in brain by Gray (50) and Peters (91). Fig. 28 shows a light cell profile considerably removed from the Mauthner cell on which three desmosome-like contacts with adjacent vesicle-filled profiles occur. At each junction there is a widening of the gap between the adjacent unit membranes with intervening dense material. There is also dense material in the cytoplasm next to each membrane. This is more prominent in the clear profile. These desmosome-like structures are, therefore, like the ones seen in some synapses by others (49, 56, 79, 83–85). Schultz, Maynard, and Pease (123) observed differentiations rather like these on profiles that they designated as astrocytes. We, however, have no basis on which to identify the profile in Fig. 28 and include it mainly to emphasize the difficulties in making such identifications on isolated micrographs.

B. Mauthner Cytoplasm and Axon

Figs. 11 to 13, 15, and 25 show the characteristic appearance of Mauthner cell cytoplasm in the formalin–osmium tetroxide-fixed preparations. It contains numerous bundles of neurotubules ~200 A in diameter with about equal numbers of neurofilaments <100 A in diameter. Endoplasmic reticulum (ER) is present in moderate abundance and sometimes shows Golgi differentiations (Fig. 11). Moderate numbers of vesicles ~400 to 500 A in diameter occur, sometimes in clusters, particularly in the Golgi regions. Numerous dense granules 150 to 200 A in diameter (presumably ribosomes) occur mainly in clusters between bundles of neurofilaments and neurotubules. Some of the ribosomes are attached to membranes but they are predominantly free. Occasionally we see peculiar myelin figure-like membrane profiles as in Fig. 13. The membranes here are generally rather loosely packed, the unit membrane strata are not displayed, and we cannot say whether they are concentrically or spirally arranged. The minimum spacing of the membranes is ~90 to 100 A. Such bodies measure ~1 to 2 μ in diameter and are not uncommon in the Mauthner cells. They may be related to the "whorl-like" structures seen by Palay and Palade (87) in the perikaryons of superior cervical sympathetic ganglion cells.

Mitochondria are present in moderate numbers in the Mauthner cells (Fig. 12). They are generally elongated and appear unusual only in that their matrix material is very dense and granular. This is, however, not peculiar to the Mauthner cell but characterizes the mitochondria everywhere in our preparations after formalin–osmium tetroxide fixation and permanganate staining (*e.g.* see Fig. 15). After prolonged permanganate staining as in Fig. 27 (left inset) the mitochondrial matrix shows dense bodies (arrows) attached to the membranes between the cristae that might perhaps be related to the "electron transport" or "elementary" particles found in fragmented

---

Figure 8 Section of myelinated and non-myelinated fibers in medulla. Note the blown-up clear glia cell process (*g*) classified as astrocytic. The nerve fiber at arrow *1* is enlarged to the lower left to show the neurotubules and neurofilaments. An area indicated by arrow *2* in the adjacent fiber is shown to the upper left at higher magnification. The area at arrow *3* is enlarged to the right to show a small myelinated fiber and a few unmyelinated fibers with neurotubules. This myelinated fiber incidentally shows the outer tongue of the myelin spiral and the inner mesaxon. Formalin–OsO_4-fixed; uranyl acetate-stained. × 9000. Left lower inset, × 47,000; left upper inset, × 62,000; right inset, × 44,000.

Figure 9 Group of myelinated fibers in medulla showing small amounts of extracellular space (*e*). The area at arrow *1* is enlarged to the left and the one at arrow *2* to the right. Formalin–OsO_4 (Millonig)-fixed; $KMnO_4$-stained. × 26,000; insets, × 55,000.

Figure 10 Neural and glial elements in medulla. The desmosome-like region at arrow *1* is enlarged above and the external compound membrane at arrow *2* is enlarged below. Note the small patch of dense extracellular matrix material at arrow *3*. Formalin–OsO_4 (Millonig)-fixed; $KMnO_4$-stained. × 26,000; insets, × 184,000.

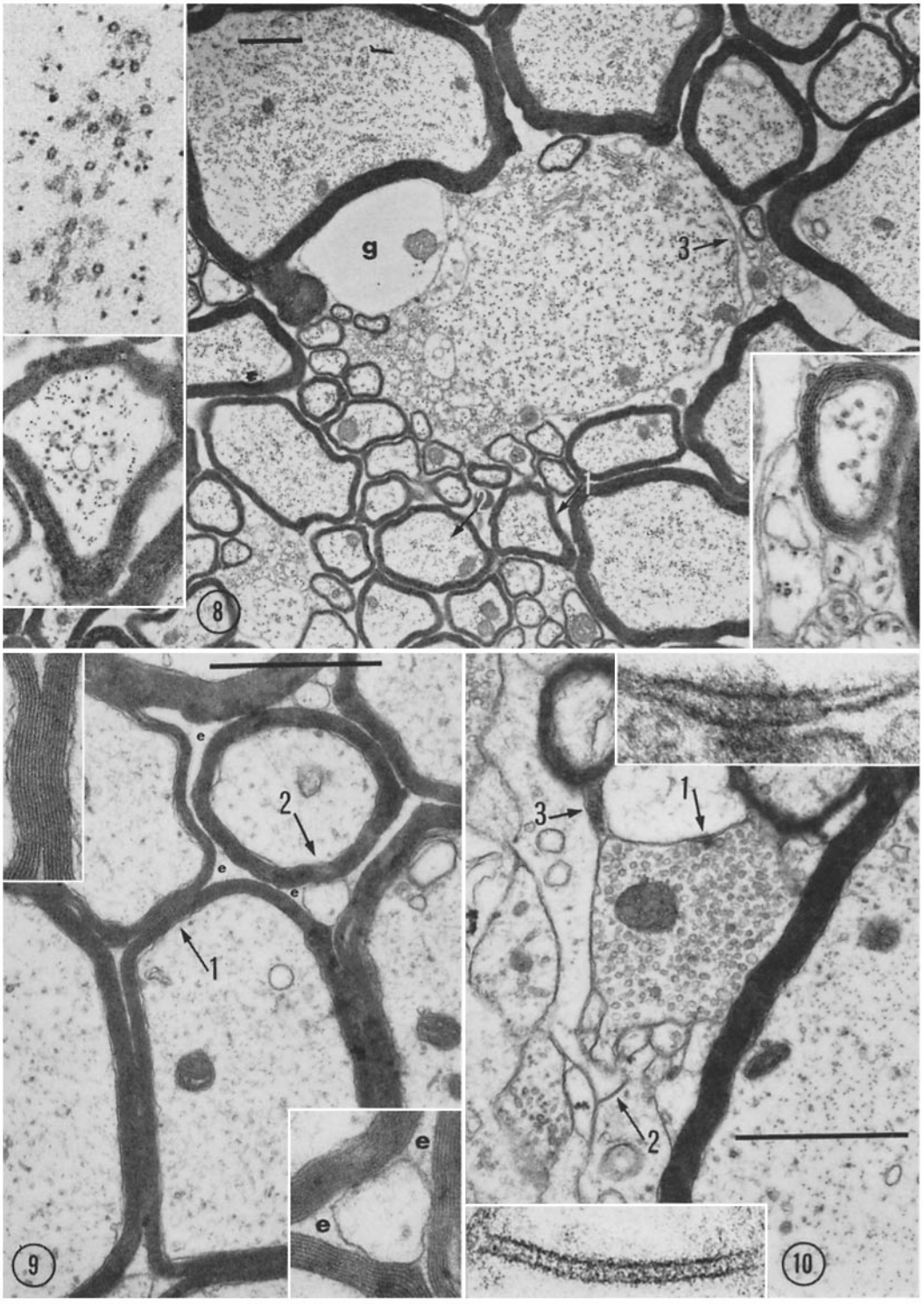
g
3
2
8
e
2
1
9
e
e
3
1
2
10

mitochondrial preparations by Fernández-Morán (35).

The Mauthner cell cytoplasm should be compared with the Mauthner axon in Figs. 35 and 36. The axon is relatively devoid of endoplasmic reticulum membranes and contains but few mitochondria. The dominant element is longitudinally oriented bundles of loosely packed neurofilaments <100 A in diameter. In between there are interspersed longitudinally oriented bundles of neurotubles ~200 A in diameter. There is a dense finely granular matrix material between the rather closely packed bundles of neurotubules. The neurofilaments show a delicate beading. Ribosomes apparently are absent in the axon although it is difficult to be sure that none are present in the dense matrix about the neurotubules. In Figs. 4, 35, and 36 the axon is obliquely sectioned but the high degree of longitudinal orientation of the neurotubules and neurofilaments is apparent.

C. The Synaptic Bed

The synaptic bed, as noted with the light microscope, is a zone about 5 μ thick (apposed block arrows, Figs. 2 and 3). With the electron microscope it is seen to contain numerous boutons terminaux, club endings, and clear glia processes, but very little myelin. In many regions, quite large amounts of dense extracellular matrix material (*) appear (Figs. 14 to 18, 23, 24, 30, and 31). We have come to look upon this matrix as a layer covering the entire soma dendrite of the Mauthner cell as a mat-like bed in which the synaptic terminals are implanted. Hence, it is an important constituent of the "synaptic bed." It is most prominent around club endings. In other nearby regions (Fig. 26) it may be reduced over wide areas to the ~100 to 150 A gap between adjacent neurites. This is usually the situation where boutons terminaux dominate.

Figs. 16 and 17 show parts of the synaptic bed with several small club endings (*C*) rather like the one at arrow *C* in Fig. 2. Note the relatively large amount of dense extracellular matrix material (*) about the endings. Fig. 18 is a similar region with mainly boutons terminaux instead of club endings. Again note the abundant extracellular matrix material (*).

Fig. 15 is a higher magnification of the synaptic bed of a lateral dendrite. A few incompletely cut synaptic endings are shown. The one to the lower left is probably a club ending but the others are not sufficiently well displayed for identification. The abundant extracellular matrix material (*) is well shown. It is a delicately fibrillar amorphous substance that is bounded on all sides by single unit membranes. However, this fundamental point can be made clearly only in regions in which all the membranes are perpendicular to the plane of sectioning and well preserved. In Fig. 15, for example, the single

---

FIGURE 11 Golgi region in Mauthner cytoplasm with the usual paired membranes and vesicles. Note the neurofilaments (*f*), neurotubules (*t*) and ribosomes (*r*). Formalin–OsO_4-fixed, $KMnO_4$-stained. × 47,000.

FIGURE 12 Portion of Mauthner cell cytoplasm showing neurotubules, neurofilaments, and a mitochondrion with dense matrix material. The ribosomes are indistinct. Formalin–OsO_4-fixed; $KMnO_4$-stained. × 24,000.

FIGURE 13 Portion of Mauthner cytoplasm showing a whorl-like membrane body about 1.5 μ in diameter. These are seen fairly frequently and their nature is unknown. A cluster of ribosomes appears to the upper left with some attached to membranes of the endoplasmic reticulum. Formalin–OsO_4-fixed; uranyl acetate-stained. × 24,000.

FIGURE 14 Section through synaptic bed showing three neural elements containing vesicles and mitochondria. Note the ~450 A vesicle with a dense content (arrow). Some of the intermingled profiles look tubular but they could be flattened vesicles. Note the dense extracellular matrix material (*) measuring over 0.6 μ between the block arrows. Formalin–OsO_4-fixed; uranyl acetate-stained. × 48,000.

FIGURE 15 Section of synaptic bed on lateral dendrite showing dense extracellular matrix material. Its thickness between the apposed block arrows is 1 μ. See Text. Formalin–OsO_4-fixed; $KMnO_4$-stained. × 45,000.

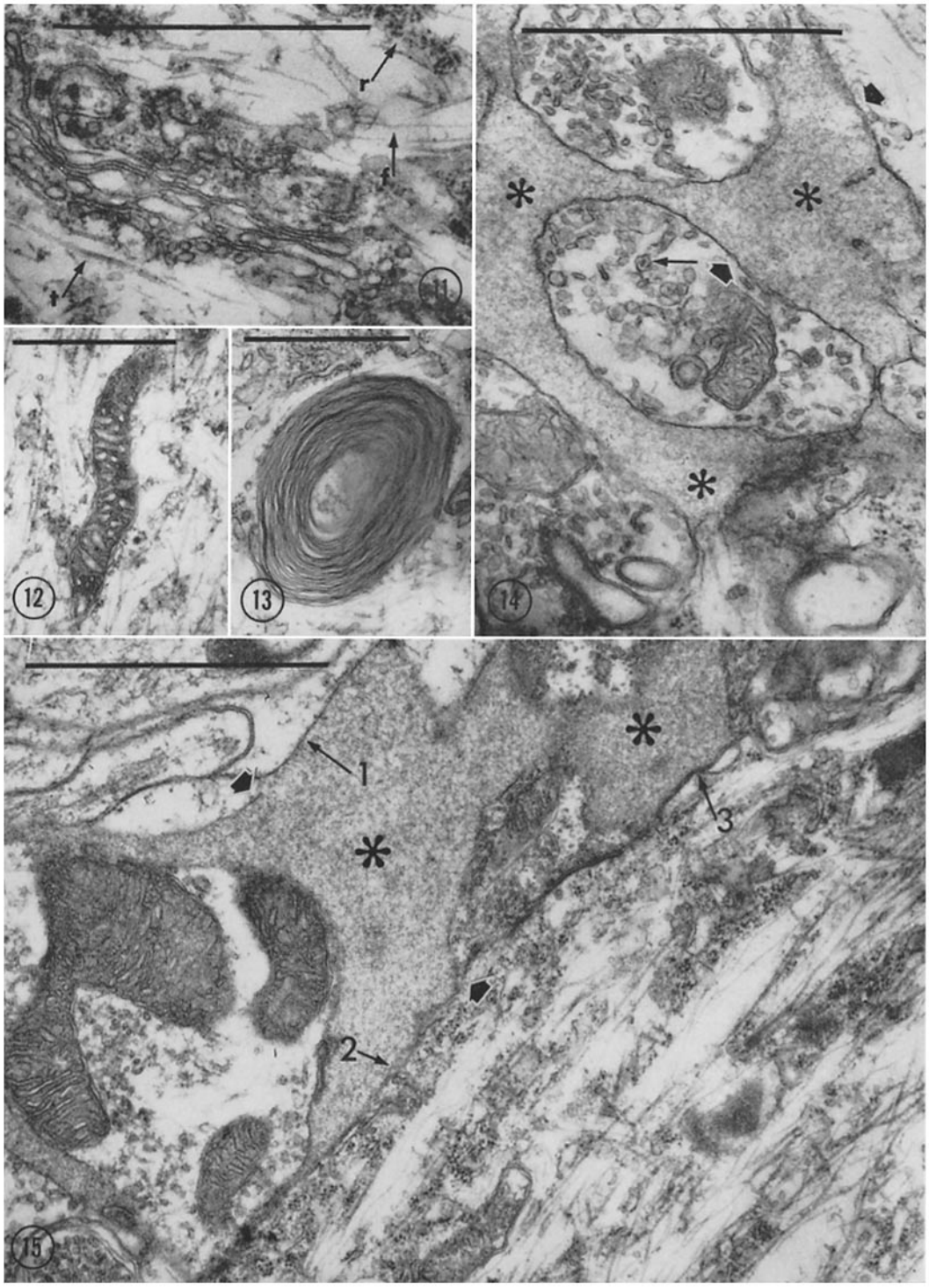
11
12
13
14
15
1
2
3

membrane bounding the matrix is clear to the upper left (arrow *1*). However, at the surface of the lateral dendrite (arrow *2*) the boundary is not clear because of oblique sectioning. Subsurface cisternae of the type described by Rosenbluth (120) complicate the picture elsewhere and even in one place (arrow *3*) give a false impression of a pair of membranes bounding the matrix. In Fig. 14 the single membranes bounding the matrix material are more clearly shown at higher power and over a larger fraction of the boundaries of the matrix. We are convinced from carefully examining all our plates that the dense matrix material (*) is always extracellular and bounded by the single unit membranes of related cellular elements. This point is again made in Fig. 31. This shows a club ending of somewhat smaller size but like the one in Fig. 30. The plane of sectioning is, however, roughly perpendicular to the long axis of the terminal axon instead of parallel to it as in Fig. 30. The section includes only a part of the unmyelinated segment of the terminal axon. The collar of extracellular matrix material (*) is unusually abundant about this particular ending, measuring a micron or more in thickness in some places. The distinction between single unit membranes and paired unit membranes is particularly clear in some regions as between the aligned opposing arrows to the lower right. A careful examination of the surface of the axon and the surrounding irregular thin overlapping layers of glia cell sheets or folds reveals many regions (smaller arrows) in which the unit membranes bounding the extracellular matrix are sectioned perpendicularly. In such places one may see clearly that only one membrane is present even though at this magnification the internal strata of the unit membranes are not displayed.

Low power survey sections passing tangentially through the synaptic bed are particularly revealing. Fig. 20 shows successively, proceeding from the left along a line running diagonally from the upper left corner to the lower right corner, three distinct zones: 1) A very small area of Mauthner cell cytoplasm just below the letter *M* to the upper left; 2) the synaptic bed with boutons terminaux (*b*), club endings (*c*), clear glia processes (*g*), and intercellular matrix material (*); 3) a very close-packed layer dominated by glia cells (*G*) containing distinct intracellular fibrillae and intimately investing all neurites. These glia cells are probably best identified as astrocytes. However, their intracellular fibrillae, perhaps because of preparatory factors, are not so heavy and distinct as the ones in the astrocytes in Figs. 21 and 22.

The amount of extracellular matrix material varies and, as stated, in some regions it is reduced about most endings to the ~100 to 150 A gap substance between adjacent cellular elements (Figs. 26 and 27). Therefore, its presence in large amounts can be assessed only if sufficient samples in different regions are taken. This also complicates any statistical assessment of its relative abundance and such an analysis has not yet been attempted.

D. Club Endings

Figs. 23 to 25 and Figs. 30 and 31 show club endings on lateral dendrites rather like the ones

FIGURE 16 Section through synaptic bed at surface of Mauthner cell to the lower left. Several small endings are shown, one of which (left *c*) is definitely identifiable as a club ending. Note the very abundant extracellular matrix material (*). Formalin–OsO_4-fixed; uranyl acetate-stained. × 6,800.

FIGURE 17 Section of lateral dendrite (below left) showing synaptic bed (apposed block arrows) with several club endings (*C*) and extracellular matrix material (*). Formalin–OsO_4-fixed; uranyl acetate-stained. × 6,800.

FIGURE 18 Section of lateral dendrite (below right) showing synaptic bed (apposed arrows). Note the vesicle-filled boutons terminaux (*b*) and extracellular matrix material (*). Formalin–OsO_4-fixed; $KMnO_4$-stained. × 6,800.

FIGURE 19 Glia cell in medulla intimately related to myelinated fibers and having ER, mitochondria, and ribosomes and containing glia fibrils (*g*). OsO_4-fixed; $KMnO_4$-stained. × 14,000.

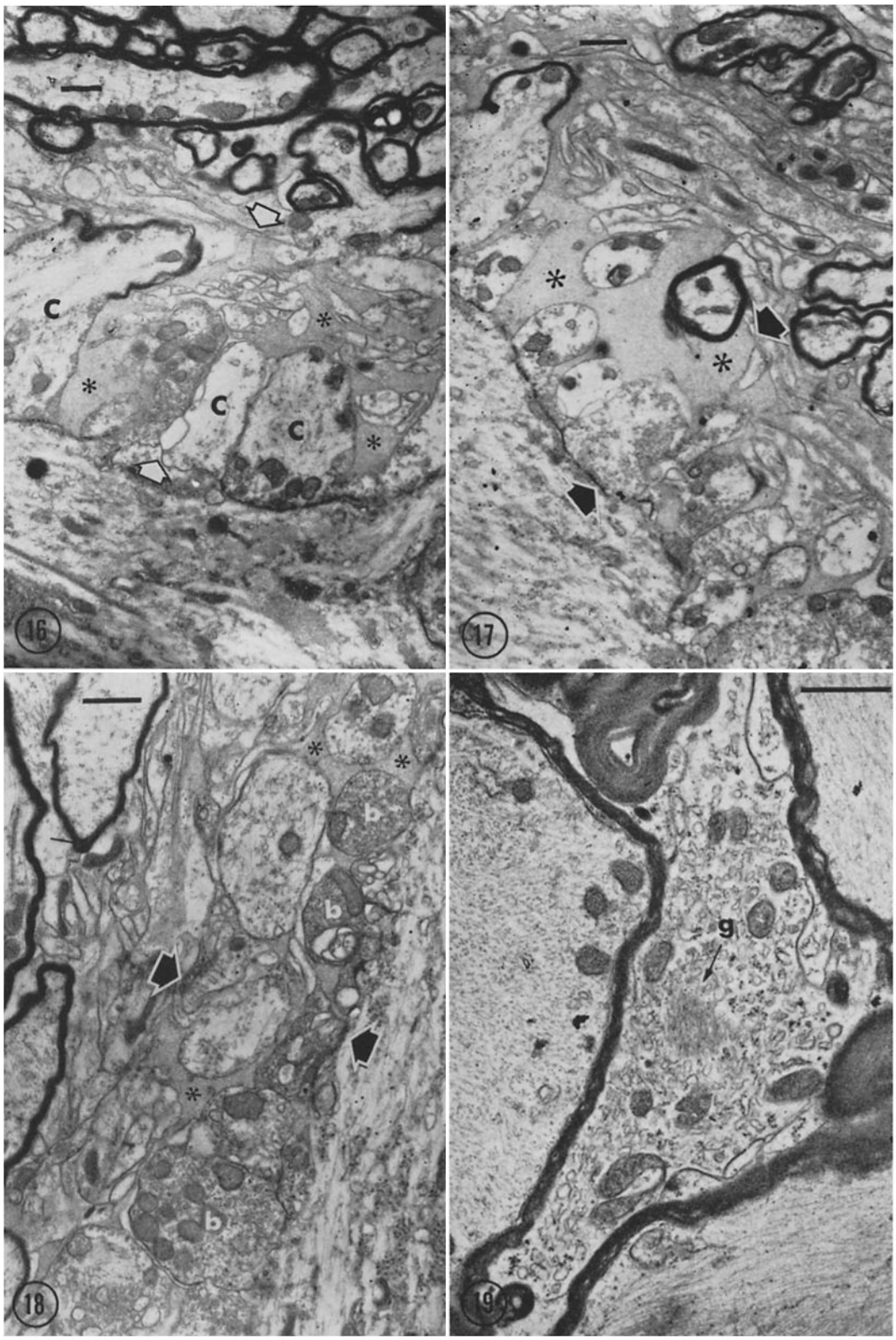
C
C
C
16
17
b
b
b
18
g
19

in Fig. 3. Although the micrographs shown are of too low power to make the point well, the terminal myelin in the club endings (Figs. 23, 24, and 30) is arranged rather like that in nodes of Ranvier in the peripheral nervous system (105, 106, 111, 128) with numerous mesaxons visible in longitudinal sections. The axon surface is free of myelin or other intimate satellite cell investments from the terminal myelin down to the synaptic contact (~1.5 μ in Fig. 24). There is a fairly prominent zone of extracellular matrix material (*) that completely covers the naked axon terminal (Fig. 24 and inset) and extends out in an interdigitating fashion among the surrounding cellular elements of the synaptic bed (Fig. 23). A single unit membrane separates the axon, the adjacent cellular elements, and the lateral dendrite, respectively, from the matrix material. The matrix material extends into the synaptic cleft (arrow in inset to Fig. 24). Clear glia processes (possibly astrocytic, see references 32, 123) often occur near the club endings as well as between boutons terminaux (*g*, Figs. 24, 25, and 30). These sometimes bulge slightly into the terminal axon (lower center, Fig. 30) or even the lateral dendrite (Fig. 25). These cellular profiles often appear completely empty of organelles and are identifiable as cellular only by their bounding membrane.

The synaptic membrane complex, SMC, (Fig. 30, arrows) in transection regularly displays a succession of segmented regions about 0.2 to 0.5 μ long in which the gap between the presynaptic and postsynaptic unit membranes is occluded with the formation of external compound membranes, ECM's, ~150 A thick. These regions we believe from serial sections and frontal views to be roughly disc-shaped. The unit membrane triple-layered pattern does not generally appear in the OsO_4-fixed material, but in the upper inset enlargement of Fig. 30 we show a synaptic disc, fixed with our standard OsO_4 method and stained with permanganate, in which all of the five strata expected of two unit membranes united in an external compound membrane (109) can be made out. This kind of pattern appears regularly in $KMnO_4$-fixed preparations (118). Partly for this reason and partly because permanganate has been shown to be a more reliable fixative than OsO_4 for membranes (108, 110, 113), we believe it is the more correct representation of the native state of the membranes. In those ECM's in which the strata of the unit membranes do not show up, the over-all thickness of the ECM is somewhat higher than 150 A. However, they do not measure over 200 A and contrast sharply with the adjacent regions of gap widening, not only by the narrowing of the gap but also by the relatively rigid parallelism of the pair of membranes. We regard the thickness values which are slightly higher than that usually found in ECM's to be due simply to failure to fix the entire unit membranes, for, if all the strata of the unit membranes are successfully fixed so that they show up as in the upper inset in Fig. 30, the thickness is close to the usual value of 150 A.

Between each of the synaptic discs of the SMC the gap between the presynaptic and postsynaptic membranes is widened to about 150 to 200 A and there is, next to the widened gaps, a slightly increased density of the cytoplasm bordering each membrane, making hazy bands ~300 to 500 A wide. This shows up best in Fig. 25. This appearance is typical of desmosomes, attachment plaques or, as Farquhar and Palade (34) refer to them, "maculae adhaerentes." The inset enlargement shows that in common with desmosomes there is also condensation of dense material in the gap between the apposed membranes making a central dense line. Since the unit membrane strata do not show up here, this paired membrane complex shows three dense and two light strata bearing some resemblance to the ones displayed by an external compound membrane, and these structures must not be confused. The dimensions alone are sufficient to distinguish clearly between these two fundamentally different junctional complexes. In the desmosome-like structure the over-all thickness of the paired membrane complex is ~300 A as compared with ~150 A for the ECM's making the synaptic discs. The fine dense and light strata in each are due to quite different things.

The axoplasm of the axon of the club ending

FIGURE 20 Oblique section through synaptic bed with small area of Mauthner cytoplasm to upper left. See text for legends. Formalin–OsO_4-fixed; $KMnO_4$-stained. × 13,000.

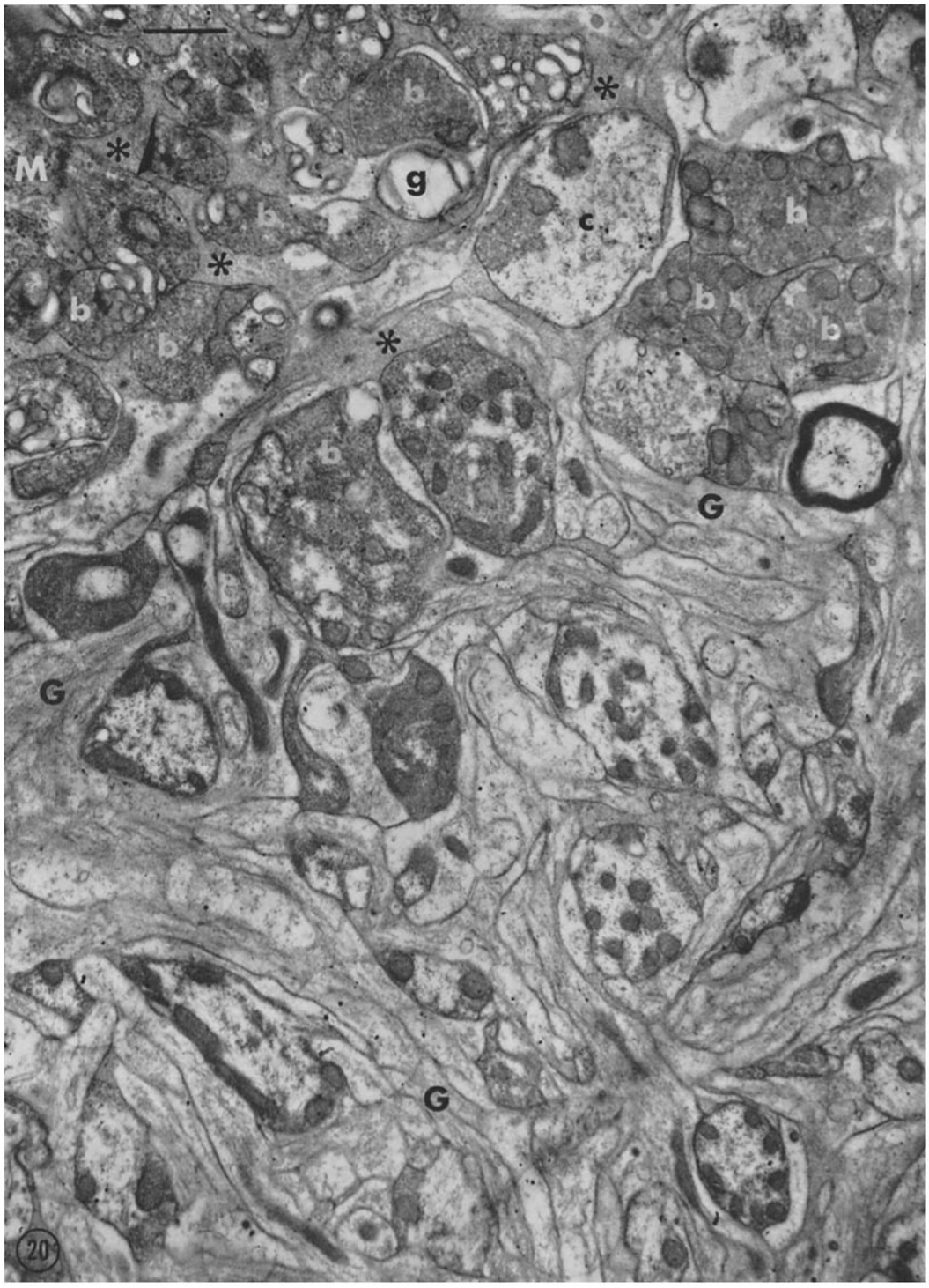
M
g
b
c
G
20

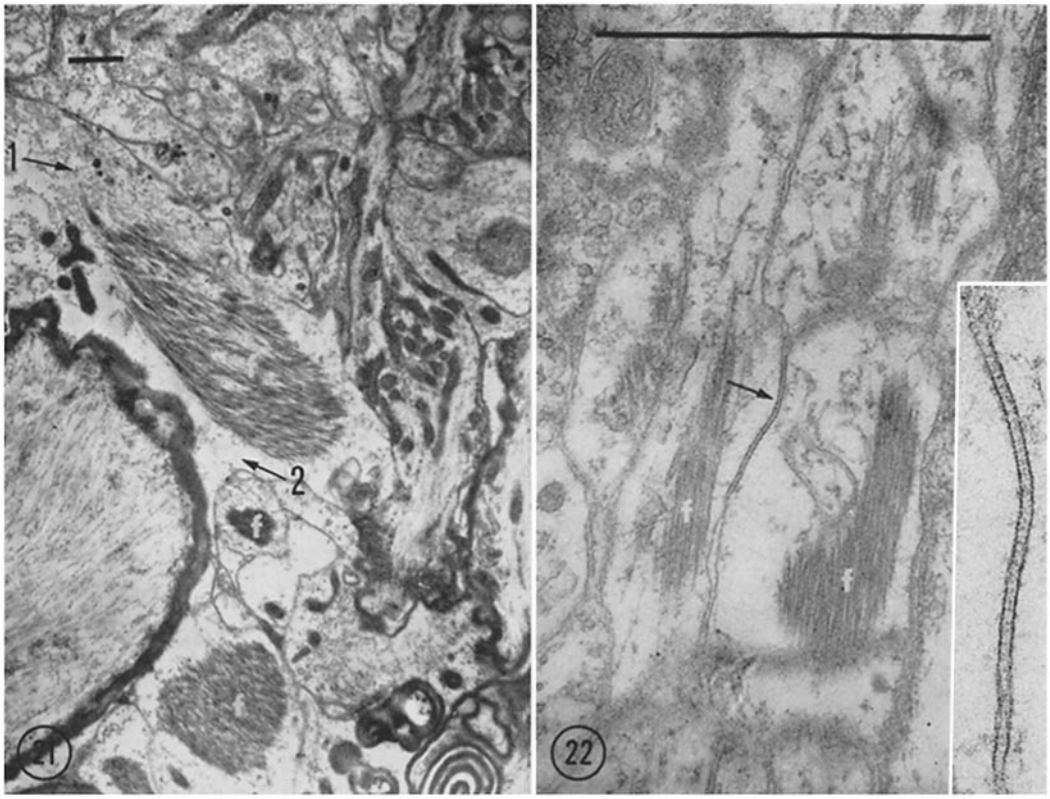

FIGURE 21 Section in medulla showing glia cells with dense bundles of intracellular fibrillae (*f*). The cytoplasm to the left of the upper fibrillar bundle (arrow *1*) contains organelles rather like the cytoplasm of axon cap cells, but to the lower center (arrow *2*) the cytoplasm appears relatively empty. This empty appearance may represent artifact. Formalin–OsO_4-fixed; $KMnO_4$-stained. × 7,000.

FIGURE 22 Section deep in the axon cap neuropil next to the Mauthner axon. Note the glia profiles with bundles of intracellular fibrils (*f*). Between two of these there is a region of close contact between membranes (arrow) in which the gap is closed making an external compound membrane. This is enlarged to the right. The over-all thickness is ~150 A and a faint trace of the outer surfaces of the united unit membranes shows as a faint dotted line appearing not unlike the intraperiod line of myelin after OsO_4 fixation. It is clear here that each of the ~30 A thick dense strata next to cytoplasm is only the cytoplasmic dense stratum of a unit membrane appearing slightly thicker than it does after $KMnO_4$ fixation. Formalin–OsO_4-fixed; $KMnO_4$-stained. × 52,000; inset, × 120,000.

contains moderate numbers of vesicles about 400 to 500 A in diameter accumulated randomly in patches over most of the axon surface beyond the termination of myelin. The vesicles are not confined exclusively to the vicinity of the SMC and bear no particular relationship to the synaptic discs or desmosome regions. The terminal axoplasm also contains large numbers of neurofilaments and neurotubules terminating perpendicular to the SMC (Fig. 30, lower inset, and Figs. 31–33). These tubular profiles in common with those seen elsewhere in neurites resemble those seen in mitotic spindles by Ruthman (121), Kane (61) and others. They are not apparent either here or in the Mauthner cells in our permanganate preparations (118). Since permanganate seems to fix lipoprotein structures almost selectively, we have tended to believe that the neurotubules are not lipoprotein in nature.

There are moderate numbers of elongated mitochondria in the club endings. They are usually arranged with their long axes roughly parallel

to the fibrillar elements. Sometimes they assume an unusual shape, bifurcating at the SMC.

E. Boutons Terminaux

The boutons terminaux (11, 12) are prominent throughout the synaptic bed and are easily differentiated from the club endings because of their distinctly different morphological characteristics (Figs. 18, 26, and 27). They are packed with synaptic vesicles and do not show neurofilaments or neurotubules. Dense particles measuring about 200 to 300 A in diameter have been observed in some (to the left in Fig. 27) and we interpret these as glycogen (96). There are numbers of contorted mitochondria. No external compound membranes have been found in the boutons endings. The gap between the presynaptic and postsynaptic unit membranes in this kind of ending, wherever the membranes are sectioned perpendicularly, regularly measures ~100 to 150 A (Figs. 26 and 27 insets). In some micrographs synaptic vesicles are accumulated next to the presynaptic membrane in the manner described by others (85, 49, 56). There may be some accumulation of dense material in the juxtamembranous cytoplasm in such regions but the densities might just as well be due to overlapping of vesicles. While some dense material may be present about the membranes, it is not clear to us whether there is any intrinsic thickening of the synaptic unit membranes in such regions. Densitometer traces in better micrographs than Fig. 26 will be helpful in deciding this point.

We have not as yet identified with certainty in our electron micrographs the axons from which the boutons spring, as might be expected if they are relatively small. Some of the smaller neural profiles to the lower right in Fig. 20 may be such axons, but serial sections will be needed to prove this.

The boutons are often closely packed over the surface of the lateral dendrite, as in Fig. 26, with the extracellular matrix material reduced to ~100 to 150 A in thickness. Occasionally one sees, between the boutons as well as club endings, single unit membrane-bounded cytoplasmic regions that are quite empty of structure and which may represent astrocytic processes if we follow the terminology of Farquhar and Hartmann (32) and Schultz, Maynard, and Pease (123). In other regions between boutons one sees accumulations of extracellular matrix material as in Figs. 18 and 26 (*). This is usually not so marked about boutons as about club endings.

F. The Axon Cap

Figs. 2 and 4 to 6 are light micrographs of the axon cap region. Fig. 29 is a low-power electron micrograph of the boundary zone of a cap. As noted above, numerous small myelinated fibers of unknown origin enter the cap. These are easily distinguished from the Mauthner axon by their size alone. One such myelinated axon (*ax*) is seen in Fig. 29, penetrating between the cap cells and losing its myelin sheath in a node-like configuration. The cap cells take over as satellite cells for the now unmyelinated axons with their membranes separated from the axon membranes by a gap of ~100 to 150 A (Fig. 29, inset enlargement). No accumulations of extracellular matrix material like that replacing the terminal myelin in club endings is seen about these fibers as they enter the cap.

As seen with the light microscope the cap cells are polygonal and form a fairly continuous sheet-like boundary with nuclei confined to the superficial zone and finger-like tapering processes extending deep into the cap neuropil. Their nuclei appear oval or round in our sections and measure about 2.5 to 3.0 μ by 6 to 7 μ in diameter. Irregular fairly light condensations of chromatin are scattered throughout the nucleus, with only a slight tendency to aggregate at the nuclear membrane. In one instance we have observed another kind of glia cell nucleus deeper in the cap neuropil. This appears in Fig. 34 at the bottom center. Its nucleus is rounder and smaller (2.0 to 2.5 μ) than that of cap cells. Its chromatin is more dense and more sharply defined as a peripheral layer, next to the nuclear membrane, extending connected folds into the central region. The cytoplasm of this cell is sparse and we believe it represents a different type of glia cell, probably an oligodendrogliacyte.

The cap cells (Fig. 29) and their processes contain numerous dense granules measuring about 150 to 250 A in diameter, either free or attached to endoplasmic reticulum. Most of these appear to be ribosomes, although some of the larger ones might represent glycogen. Some of the smaller extensions of glial elements deep in the cap are derived, we believe, from the cap cells. They often contain typical astrocytic filaments (Fig. 22) like those in the glia cells outside

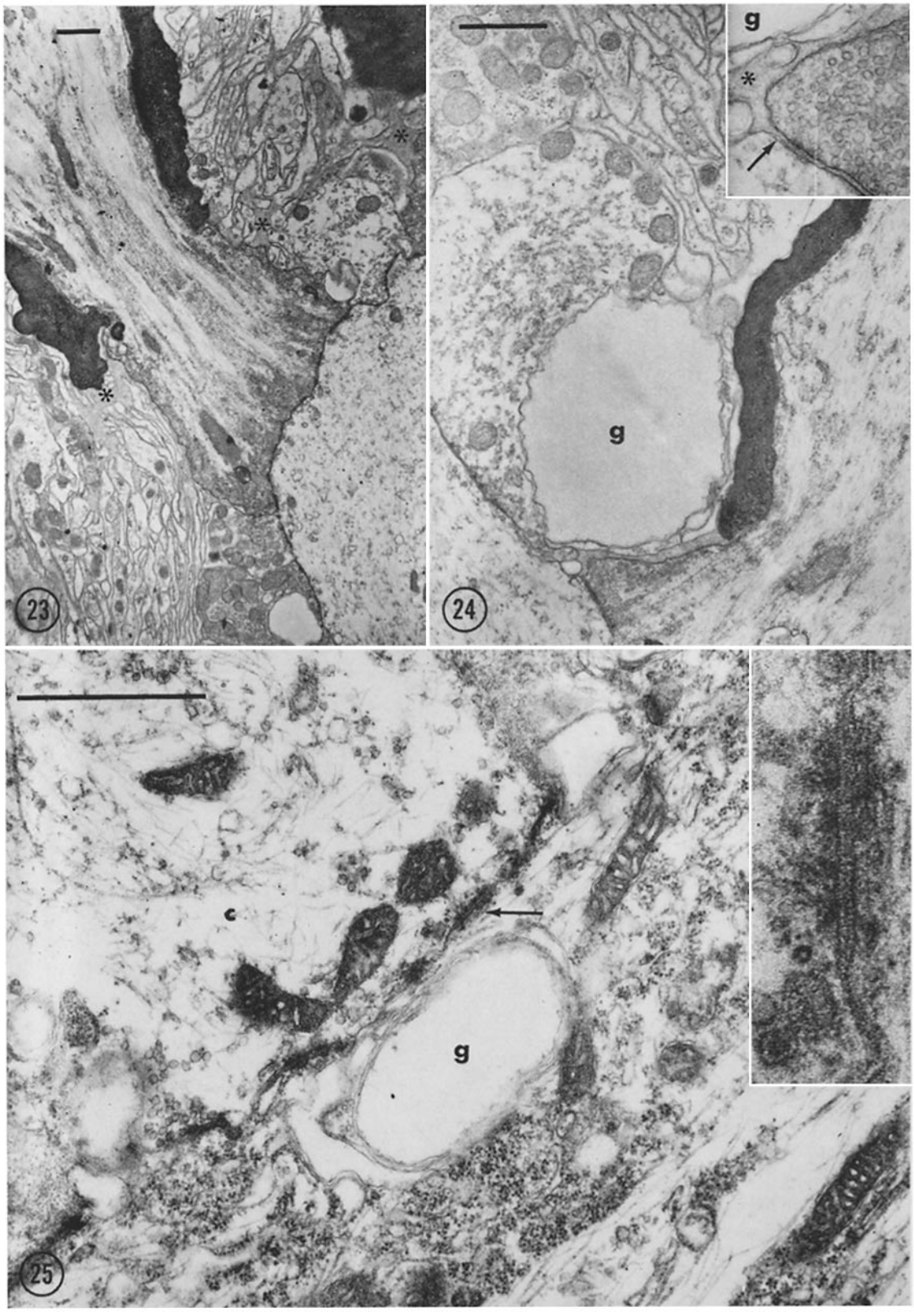
23
24
g
25
c
g

the cap in Figs. 19 and 20. The glia cell in Fig. 19 outside of the cap region is closely related to myelin and contains glia filaments as well as the ribosomes and ER characterizing the cap cells. This cell would seem to be best classified as an astrocyte and, if so, its similarity to the cap cells makes it seem likely that the cap cells also are astrocytes. In Fig. 21 we show some glia cells, not far from the Mauthner cell, that have clear bundles of glia filaments that would support their classification as astrocytes. They are closely related to myelin and in some regions display clear cytoplasm almost free of structure (arrow *2*). To the upper left (arrow *1*), however, there is a transition zone, in one of these cells, to a region in which the cytoplasm contains organelles and gives an appearance rather like that given by the cap cells. While it seems reasonable to us on the basis of the above features to classify the cap cells as astrocytes, the proof of this must await the demonstration of glia fibrils in indubitable cap cell cytoplasm. We believe that the fibrils are present mainly in the smaller extensions of cap cells and that, as they appear, the ribosomes and ER are reduced in amount, so that all the distinguishing features are not frequently seen in one region. Hence, our identification of the cap cells as astrocytes is not yet certain.

The over-all picture of the cap region (Fig. 34) is one of a very dense, tightly packed neuropil consisting of neural and glial processes, arranged in a complicated, interwoven fashion with transected elements measuring most often a few tenths of a micron in diameter but reaching several microns in some cases. The largest ($\sim$3 to 4 μ) we believe generally to be axons or dendrites. In some low power micrographs we can see numerous desmosome-like regions. One of these is shown at the arrow in the upper left inset in Fig. 34.

Throughout the cap neuropil there are frequently seen dense, irregularly shaped regions measuring a few tenths of a micron across. Several of these are visible in Fig. 34 (unmarked arrows). At higher magnification (Fig. 34, right upper inset of circled area, and left inset from another micrograph) these are found to be dense, extracellular matrix material like that in the synaptic bed.

Some of the neurites in the cap region show great accumulations of mitochondria. Vesicles occur in large numbers in some of the profiles and some contain very dense granules $\sim$600 to 1000 A in diameter (*gr*, Fig. 34) which we have not yet identified.

G. Nodes

We have incidentally encountered several nodes (Figs. 37 and 38) in the medulla. These resemble, in agreement with the findings of other observers (81, 129), nodes of Ranvier found in the peripheral nervous system. The unmyelinated part of the axon is bounded by a single

FIGURE 23 Low power view of club ending. Lateral dendrite is to lower right. Formalin–OsO_4-fixed; uranyl acetate-stained. × 6,800.

FIGURE 24 Higher power view of edge of a club ending below. Note the empty large glia process (*g*) to the left next to the boutons. This is bounded by several thinner sheet-like glia processes (inset) that are intimately related to myelin above. Note the thin but clear-cut layer of extracellular matrix material (*) extending into the synaptic cleft (inset). The inset enlargement is from a serial section. Formalin–OsO_4-fixed; uranyl acetate-stained. × 14,000; inset, × 33,000.

FIGURE 25 Section of a club ending (*c*) in a Mauthner lateral dendrite (*M*). The clear area (*g*) in the lower center probably represents a smaller clear glial process bulging into the Mauthner cell and pushing under the synaptic membranes. The synaptic discs are not well shown here but the intervening desmosomoid regions show up well. The one designated by the arrow is enlarged to the right. Note the accumulations of dense material in pre- and postsynaptic neuroplasm next to the synaptic membranes and the condensed stratum of dense material bisecting the intermembrane gap. One can see the narrowing of the gap as the synaptic discs are entered above and below but here the membranes do not show up well partly because they are obliquely sectioned. Formalin–OsO_4-fixed; $KMnO_4$-stained. × 30,000; inset, × 120,000.

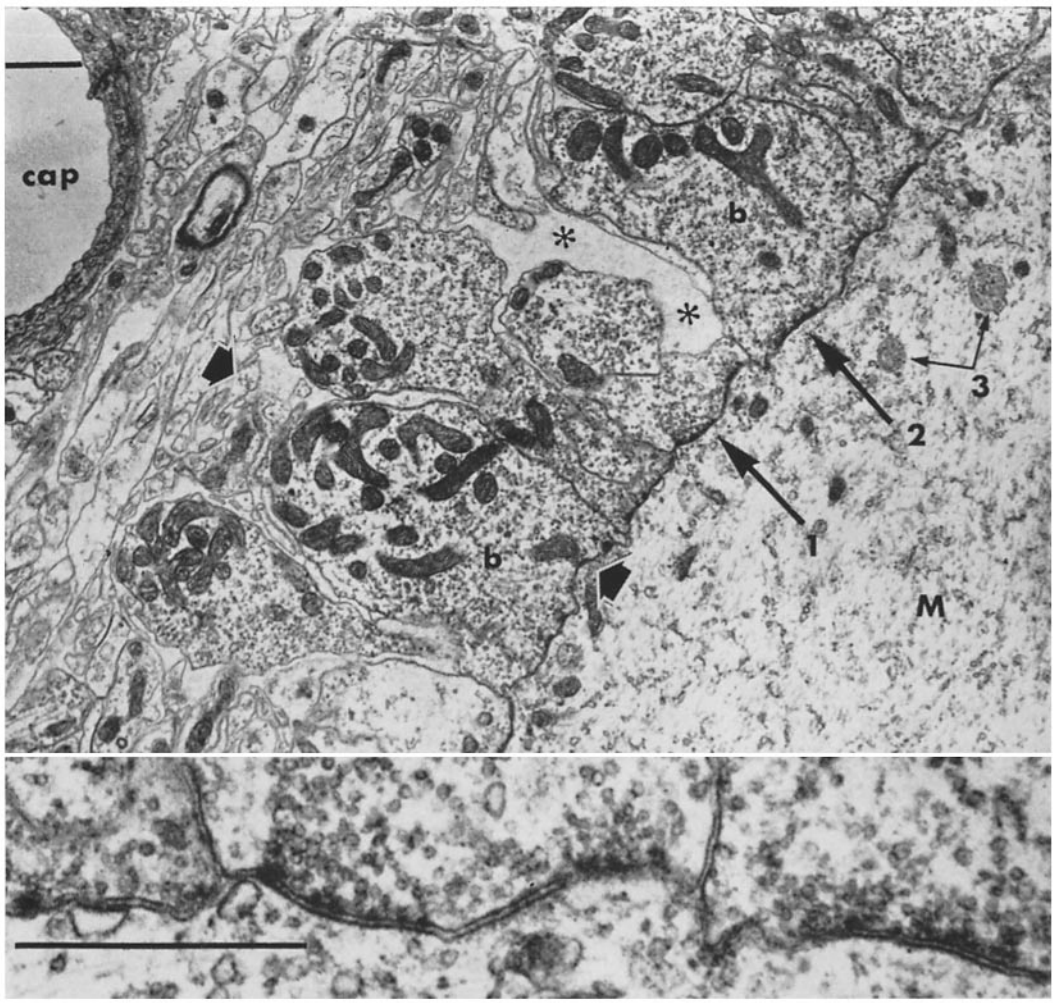

FIGURE 26 Section of lateral dendrite (*M*) with the synaptic bed containing many close-packed boutons terminaux (*b*) filled with synaptic vesicles and mitochondria. A capillary lumen (*cap*) lies to the left above. The opposed large block arrows designate the synaptic bed. A small amount of extracellular matrix material (*) is present between some of the boutons. The inset below shows the synaptic membrane complexes designated by arrows *1* and *2*. Note the accumulations of synaptic vesicles next to the presynaptic membranes. Arrow *3* points to multivesicular bodies in the lateral dendrite. 2.5 per cent OsO_4-fixed; $KMnO_4$- and lead-stained. × 10,000; inset, × 39,000.

unit membrane.[4] The node in Fig. 37 is one of a series of serial sections and we are convinced here that there is an extracellular space next to the unmyelinated part of the node. This preparation was fixed with our standard OsO_4 fixative and we believe that it may be for this reason that no appreciable extracellular matrix material shows up. Only a few delicate strands (arrows) persist. However, sometimes the matrix does show up even with this technique. In Fig. 38, another node is shown after fixation with the formalin–

[4] This is fairly clearly evident in Fig. 38, but in Fig. 37 to the upper left the section gives an impression of two membranes bounding the axon. Our serial sections of this node showed that this is not so. The lower dense line is probably due to an axon filament lying close to the surface. We have included this micrograph for the reasons indicated in the text, and it is not selected to show the characteristics of the axon membrane, a topic that will have to be dealt with separately.

OsO_4 technique. Here, in the analogous space next to the axon, dense extracellular matrix material (*) like that in the synaptic bed shows up clearly. The demonstration of the matrix material provides a good reason for believing the perinodal space to be real. Our findings on this point are in agreement with the conclusions of Metuzals (81).

DISCUSSION

Many features of CNS ultrastructure have been touched upon in our findings, but there are two subjects which we would like to discuss in some detail, the problem of the extracellular space of brain and questions relating to synapses. The belief among electron microscopists that the extracellular space of vertebrate brain is confined to the very thin ~100 to 200 A gaps between adjacent neural elements is now well established. To be sure, the published electron micrographs of others occasionally have shown appreciably large spaces between synaptic elements at neurone surfaces (84, 85, 51) but they have generally been regarded as artifact. This has seemed reasonable partly because the spaces have appeared empty of structure and partly because it was evident sometimes that the surfaces bordering the spaces would fit together like the pieces of a jigsaw puzzle, suggesting that they had separated during or after fixation. Only Blackstad (9) and Blackstad and Dahl (10) have chosen to take seriously any such spaces and their interpretations stand as an isolated exception. We believe we have presented in the literature the first evidence that strongly suggests that any such spaces be regarded as real, mainly because we have demonstrated within them a definite extracellular matrix material that could hardly arise as a preparatory artifact. Our results are, to be sure, confined to one specific case, and a general survey will be necessary before any generalities can be made. Nevertheless, since our results provide a clear-cut exception to the generally accepted concept of minimal extracellular space, it seems appropriate to examine briefly some of the evidence on which this important concept is based.

The minimal extracellular space viewpoint seems to have been explicitly recorded first by Wyckoff and Young in 1954 (139) and 1956 (140). Dempsey and Wislocki (25) and Maynard and Pease in 1955 (78) and Dempsey and Luse in 1956 (24) indicated that there might be no more than the narrow gap between adjacent cellular elements in contact to represent extracellular space. Subsequent papers by Schultz, Maynard, and Pease (123), Farquhar and Hartmann (32), and Horstmann (58) in 1957, and Horstmann and Meves (59), and Gray (49) in 1959 have supported the notion of minimal extracellular space in brain. Horstmann and Meves attempted a quantitative study of the extracellular space in certain regions, and estimated a mean volume percentage of no more than 5 per cent.

A less direct method of discerning the amount of extracellular volume in the central nervous system has been that of administering substances which supposedly remain in the extracellular compartment, and measuring the extent of their uptake. This has been done *in vitro* by incubation of brain slices with a substance to be measured, and *in vivo* by injection into the animal. Early studies were done with chloride ions, which were assumed to be distributed in the brain only extracellularly. Values of 30 to 40 per cent were obtained for chloride space by Manery *et al.* (73–75). It has been agreed since that chloride does enter at least some of the cells, and that these values are much too high (1, 2). *In vitro* studies, such as that by Allen (1) which yielded an inulin space of approximately 15 per cent, might be questioned because of possible brain swelling and distortion. Davson and Spaziani (19) calculated an extracellular space of 14 to 22 per cent, using I^{131}, sucrose, and *p*-aminohippuric acid (PAH), also relying on an *in vitro* method. More recent *in vivo* studies, however, report values close to 5 per cent for what is thought to be the true extracellular volume. Woodbury *et al.* (137, 138) and Barlow *et al.* (4) found the sulfate space to be about 4 per cent. Similar values were reported by Woodbury for inulin (137), by Streicher and Press (127) for thiocyanate, and by Reed and Woodbury (93) for I^{131}.

Thus we find that there is at present more agreement between the biochemical and the morphological estimations of the amount of extracellular space of the brain than there was at first. However, a distinct note of caution must accompany this agreement. First, neither discipline has employed methods of high intrinsic accuracy. The small samples represented by electron micrographs pose difficult statistical problems, and the chemical methods are limited by

unknowns such as penetration of the substances into cells and incomplete passage from blood to brain (28, 65). Secondly, while the older indirect studies doubtless suggested values that were too high, the more recent *in vivo* experiments may have led to values that are too low because of blood-brain barrier problems. Our results suggest that the older estimates from electron microscopy also were too low for two reasons. First, lakes of extracellular matrix larger than the ~200 A gaps between cells might exist in many places other than those reported in this paper. Secondly, there may be an artifact of fixation whereby certain kinds of cells swell differentially, making the extracellular volume appear less since the total volume of the brain is rigidly restricted. Several experiments (45, 63, 71) suggest that one kind of glia cell, called astrocytes by most observers (31, 32, 78, 79) but oligodendroglia by Luse (68–71), displays a definite tendency to take up water very readily if subjected to trauma before fixation. Since these cells in the untraumatized experimental controls did not show such extreme swelling, it seems reasonable to agree that the extreme swelling was due to the prefixation trauma. This says nothing, however, about the possible effects of the trauma of fixation itself. Perhaps the less dramatic swollen appearance that astrocytes so often display in electron micrographs is related to some extent to an unusual susceptibility to the trauma attending fixation. These cells, even in apparently well fixed normal preparations, often have a completely empty cytoplasm that makes one very suspicious of artifact (*e.g.*, Fig. 24). Some of the previous observers appear to have reasoned that since the surrounding cells look well fixed, so must be the astrocyte. However, it may well be that when these cells look poorly fixed by the usual criteria, they are poorly fixed. In support of this viewpoint we have seen transitions, in the same cell, from regions with a swollen watery appearance to regions that look better preserved and are fairly well filled by organelles (Fig. 21). Thus, selective astrocyte swelling during fixation could have the effect of decreasing to some degree the amount of extracellular space thereby making it different from that existing *in vivo*. In the experiments of Van Harreveld (130) and Van Harreveld and Schadé (131) on cortical impedance changes after asphyxiation, these changes that were explained by the authors as due to neuronal swelling are, perhaps partly explainable by astrocytic swelling. This is not to say that we believe that this alone can account for such very high values for brain extracellular space as the extreme ones (~30 per cent) suggested by these authors. This kind of argument, based on selective swelling of some cellular element, whether applied to astrocytes, neurones, or other types of cells, could have only a limited application if we assume the presence in any hypothetical *in vivo* spaces of a matrix material like that we have demonstrated about the Mauthner cell. Selective swelling of cells into these spaces could only occur to the extent to which the matrix material could

FIGURE 27 Section of bouton. The lateral dendrite lies to the right. Numerous vesicles are seen near the lateral dendrite and to the left these are replaced by aggregates of dense granules of similar size. These are interpreted as glycogen. The indicated portion of the synaptic membrane complex is enlarged above. The unit membranes do now show up but the ~100 to 150 A gap is evident. The mitochondria show dense aggregates of material in the matrix between the cristae (arrow) that may be related to the electron transport particles described by Fernández-Morán (35). Formalin–OsO_4 fixation. $KMnO_4$ stain. × 28,000. Right inset × 170,000; left inset, × 210,000.

FIGURE 28 Clear cell process in medulla with three desmosomoid membrane differentiations between it and three profiles with many vesicles. The process contains one mitochondrion and suggestive tubular profiles (arrows *1*) and dense filaments or granules (arrows *2*). Formalin–OsO_4 (Millonig)-fixed; $KMnO_4$-stained. × 54,000.

FIGURE 29 Axon cap cell. Note the axon (*ax*) losing its myelin (arrow) as it penetrates the cap. The inset enlargement shows the ~250 to 300 A paired membrane (arrow) between the satellite cap cell and the axon. Note the numerous ribosomes in the cap cells and the oval nuclei with lightly dispersed chromatin. OsO_4-fixed; $KMnO_4$-stained. × 5,400; inset, × 20,000.

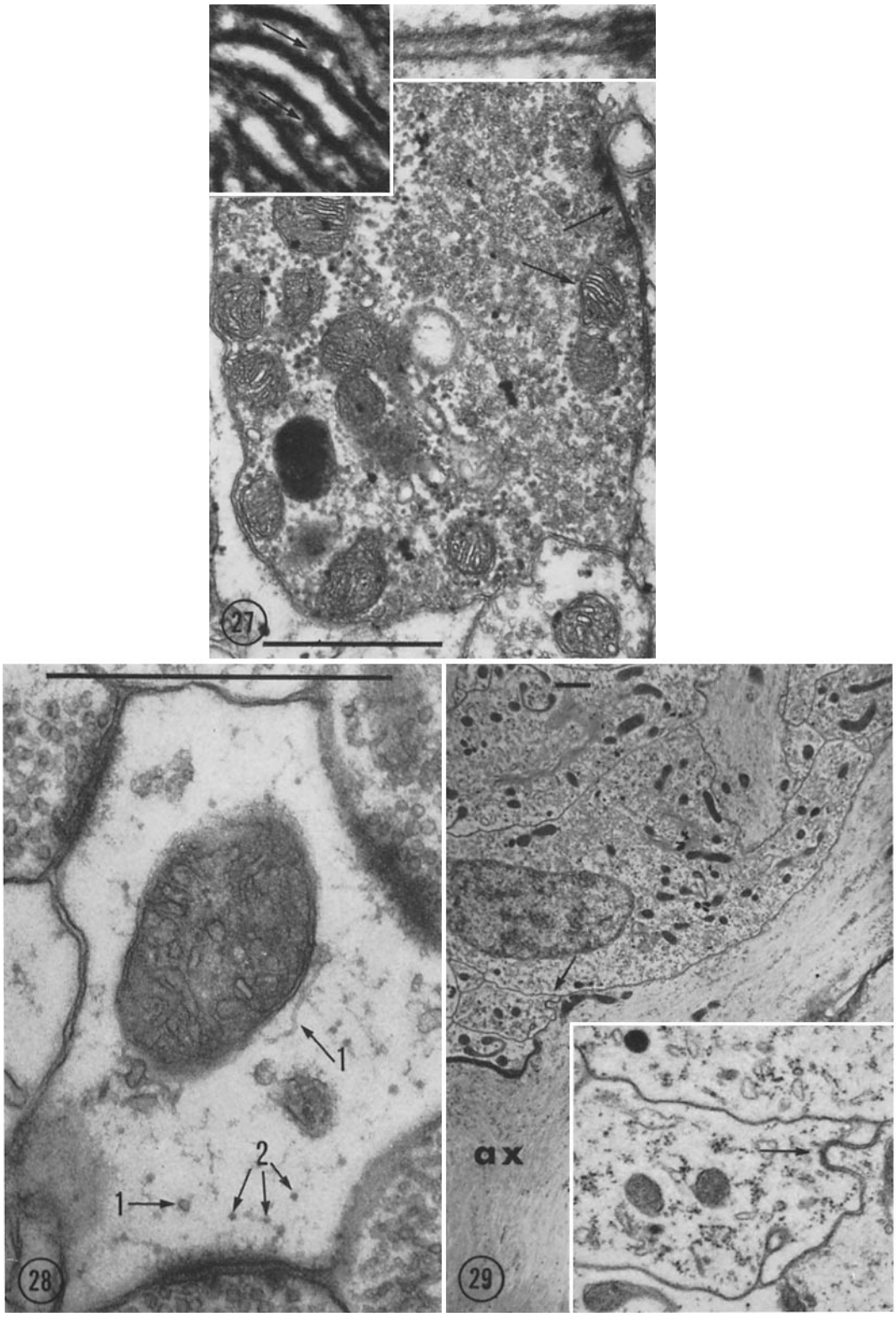
27
28
1
2
1
ax
29

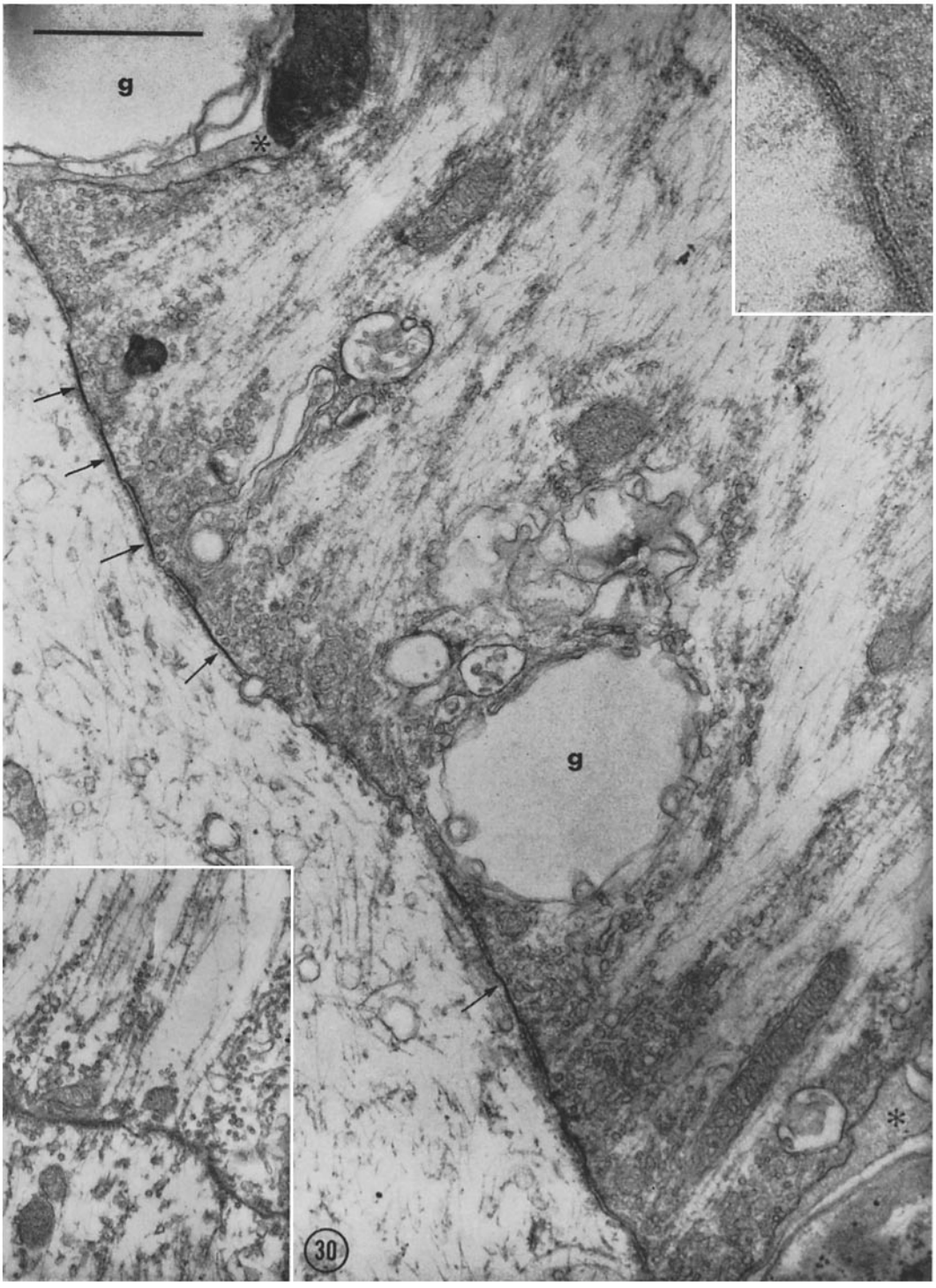
g
g
30

be dehydrated without becoming so dense as to restrict further swelling. While this might allow for considerable change since the matrix may be very highly hydrated, it seems probable that other factors need to be invoked to explain the findings of Van Harreveld and Schadé.

Light microscope techniques, although used extensively in the past in assessing the over-all volume of extracellular space in brain, have not often been used in attempts to define localized accumulations of matrix material such as we have found about Mauthner cells. The only study known to us that is relevant to this problem is one by Gasic and Badinez (42). These authors, using a combined enzymatic and histochemical technique (see reference 43), have produced light microscope evidence suggesting the presence of a thin layer of a Hale-positive mucopolysaccharide around the soma dendrites of many neurones in frog brain. We have applied the periodic-acid–Schiff technique to the Mauthner cell in formalin-fixed, paraffin-embedded material and obtained a strongly positive reaction in the synaptic bed. This could be due to the matrix material. However, the axon cap, where there is very little matrix, is also strongly PAS-positive, serving to emphasize the difficulties in making interpretations, from such methods, about the chemical nature of the reacting material (57) in any given location. However, the Gasic and Badinez technique, utilizing enzyme-treated controls, offers a possibility of greater specificity.

Apart from the chemical nature of the matrix material, we have found this material in extracellular reservoirs around bare axon surfaces at synapses and nodes, places at which one might expect major exchanges of ions during nerve impulse propagation. Frankenhaeuser and Hodgkin (37) and Ritchie and Straub (98) have produced, independently, physiological evidence that the thin hydrated film of gap substance between nerve membranes and satellite cell membranes in unmyelinated nerve fibers can act as an immediate donor and receiver of the ions exchanged between axoplasm and the outside during impulse propagation. Their results, however, showed that the balance of the ions in these small spaces can and must be restored rapidly by diffusion from extracellular reservoirs located no more than a few microns away, with the ions moving, in the cases studied, along mesaxon clefts. It seems reasonable to suggest that the reservoirs of extracellular matrix material about Mauthner cell synapses and nodes may serve not only as immediate sources and sinks for ion currents, but also for restoration of ion imbalances in the thin intermembrane gaps in the vicinity of the reservoirs up to a radius of a few microns. The reservoirs in turn could be supplied slowly by diffusion from capillaries through the thin intermembrane gaps between glia cells and neurites, provided all of these are not completely occluded (51, 91). Alternatively, the reservoirs could be supplied by astrocytes as suggested from previous work because, in the absence of sizable reservoirs of extracellular material in brain, astrocytes seemed a logical candidate for the functional role normally assumed by extracellular material in other tissues. This hypothesis, giving the astrocytes the role of an ion reservoir, requires the existence of a three compartment, two membrane system for the events of nerve impulse propagation; *i.e.*, neuronal and astrocytic cytoplasm, their cell membranes, and the extracellular gap. However, for the places around the Mauthner cells where increased extracellular reservoirs are found, it seems unnecessary to postulate such a three compartment, two membrane system, since the neuronal cytoplasm, the extracellular reservoir (or narrow gap in the

FIGURE 30 Part of a club ending at higher power showing synaptic discs (arrows). Note the mitochondria terminating perpendicular to the SMC along with neurotubules and neurofilaments that are better shown up in the left lower inset. The synaptic vesicles bear no particular relationship to the SMC or synaptic discs. The main figure was formalin–OsO_4-fixed and uranyl acetate-stained. The upper inset shows a higher magnification picture of a synaptic disc from a preparation fixed with OsO_4 only and stained with $KMnO_4$ in which all the unit membrane strata show up. Here the external compound membrane measures ~150 A. The lower inset shows another club ending with the presynaptic axon above. Note the neurotubules and neurofilaments terminating perpendicular to the SMC. This preparation was OsO_4-fixed and $KMnO_4$-stained. × 25,000. Upper inset, × 170,000; lower inset, × 17,000.

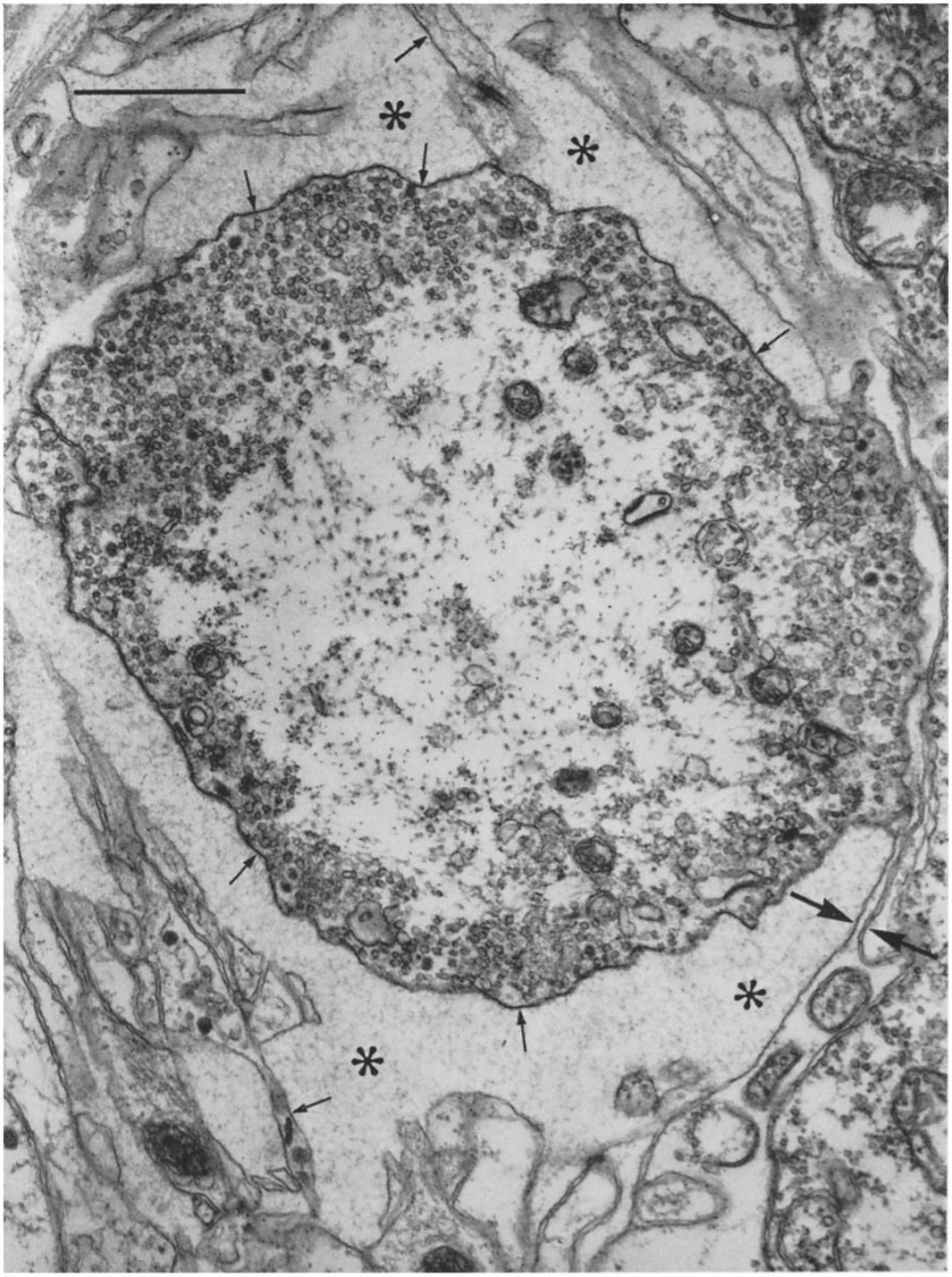

FIGURE 31 Cross-section of a club ending on a lateral dendrite. The plane of the section passes through the non-myelinated portion of the axon. Note the numerous synaptic vesicles preferentially accumulated in the peripheral zone of axoplasm. Neurotubules and neurofilaments are prominent in the central core zone. Mitochondria are seen as small round profiles in keeping with their perpendicular orientation to the SMC. Note the collar of extracellular matrix material (*) surrounding the axon. The opposed arrows include a sheet-like fold of glia cytoplasm and the distinction between single and paired unit membranes is clearly made. The other arrows point to regions in which the matrix material is clearly bounded by single membranes. In other regions the membranes are blurred by oblique sectioning. Numerous glia folds surround the matrix and other synaptic endings with vesicles appear to the right above and below. Formalin–2.5 per cent OsO_4-fixed; $KMnO_4$- and lead-stained. × 26,000.

vicinity of a reservoir), and the neuronal cell membrane may be sufficient. It remains to be seen, from further studies of brain structure, to what extent this viewpoint has geenral significance.

The structural differentiations occurring in synaptic regions have already been studied extensively by electron microscopists. For example, and Ladman (64) have studied the retinal rod synapses.

One of the most difficult problems in the correlation of structural and functional concepts is that of accurately defining the synapse. One may define a synapse in physiological terms as a region in which functionally effective neural

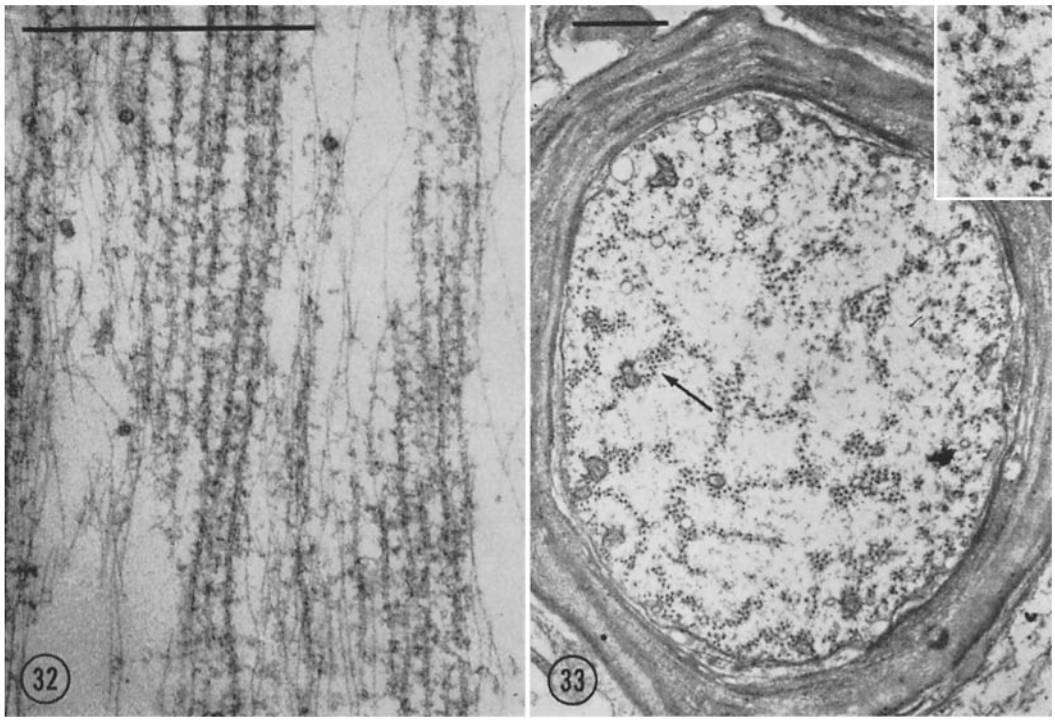

FIGURE 32 Higher magnification micrograph of axoplasm of a club ending in longitudinal section showing neurofilaments and neurotubules. OsO_4-fixed, $KMnO_4$-stained. × 38,000.

FIGURE 33 Transection of the preterminal axon of a club ending near the synaptic bed. Note the neurotubules. One bundle of these is enlarged in the inset. OsO_4-fixed; $KMnO_4$-stained. × 14,000; inset, × 53,000.

invertebrate synapses were studied by De Robertis and Bennett (26), Robertson (99–104, 114), Estable *et al.* (30), Hama (55), De Iraldi *et al.* (20), and by Gerschenfeld (44). Vertebrate CNS synapses have received attention from Palade and Palay (83), Palay (84, 85), Gray (49, 51, 52), De Lorenzo (22, 23), Gray and Whittaker (53, 54), Whittaker and Gray (133), Schultz, Maynard, and Pease (123), Boycott, Gray, and Guillery (14), and Hamlyn (56). Degeneration of CNS synapses has been studied by Colonnier and Gray (18). In addition, Sjöstrand (124) influences are transmitted from one neuron to another. This requires the fairly close contiguity of pre- and postsynaptic cells at some loci. Such loci were defined by light microscopy as regions of discontinuous membrane contact and a definite physiological correlation was made by Cajal (16) when he ascribed to such regions the function of synaptic transmission. The electron microscope has shown that in such contact regions, which may extend for many microns, the pre- and postsynaptic membranes are for the most part separated by a cleft ~150 to 200 A in width.

Within these relatively broad areas of contact, small localized membrane differentiations in the range of a few tenths of a micron in size have been defined, and a unique role for them in synaptic transmission has been imputed. However, we do not know to what extent the intimate physiological events underlying synaptic transmission are localized or diffuse in terms of tenths of microns. Hence we cannot possibly say with any certainty to what degree any particular small structures within synaptic regions many microns in extent may be uniquely involved in the physiological events.

By leaving aside such problems of the exact sites of nerve impulse transmission at synapses and dealing only with the intimate structural differentiations that are found, certain general concepts of synaptic ultrastructure have been developed. First, the neurone doctrine of Cajal, whereby the integrity of pre- and postsynaptic neuroplasm at synapses is maintained by the intervention of a distinct membranous structure between them, has been abundantly confirmed and each of the two synaptic membranes has been identified as a unit membrane (49, 23). The gap, or synaptic cleft, between the two membranes in some regions has been found to be slightly widened to ~250 to 300 A as compared with the usual ~150 to 200 A gap between adjacent cell membranes. Gray (49), following the practice of earlier workers (83–85), focused attention on certain desmosome-like focal differentiations at axodendritic and axosomatic contact regions and classified cortical synapses in rats into two types (I and II). Type I is characterized by the presence of desmosomoid regions about $\frac{1}{2}\mu$ long in transverse section and has a cleft ~300 A wide containing a thin condensed stratum of gap substance lying closer to the postsynaptic membrane. There is a condensation of presynaptic vesicles and a distinct accumulation of dense material in postsynaptic cytoplasm next to the membrane. Type II shows smaller desmosomoid regions about half as long in sections in which the synaptic cleft is narrower (~200 A) and contains no intervening dense stratum between the membranes. The postsynaptic dense material is less marked and the presynaptic vesicles are less numerous. Both types occur on dendrites but Type I is characteristic of dendrite spines and Type II of axosomatic synapses. In Hamlyn's (56) material the Type II desmosomoid regions show symmetrical accumulations of dense material in pre- and postsynaptic axoplasm and because of this fairly small difference in structure he regarded them functionally as "attachment plaques" (desmosomes) rather than synapses. The regions between the synaptic discs in our Fig. 25 have similar structural features. Should they then be regarded functionally as attachment plaques?

This question brings us back to the very serious problem, already alluded to, of deciding whether or not any particular structural entities that may be observed in anatomically defined synaptic regions have anything crucially important to do with the physiological processes of synaptic transmission. Schultz, Maynard, and Pease (123) have already brought up this problem when they claimed to show regions of differentiation in brain like those believed by most observers to be characteristic of synapses at contacts between neural processes and cell profiles that they identified as astrocytic. This has been regarded by some as casting doubt upon the unique involvement of such junctional complexes in synaptic transmission, by some as evidence of synaptic transmission to glia cells, and by some as an example of incorrect identification of glia cells. While there are some differences such as their asymmetry, these desmosomoid regions in synaptic areas resemble closely desmosomes seen elsewhere. It has seemed reasonable to ascribe to the very similar structures in organs other than brain a function of holding cells together that might otherwise be pulled apart mechanically because of a sparsity of supporting connective tissue elements.

FIGURE 34 Low power view of cap neuropil showing interwoven glial and neural elements. The latter often contain vesicles or many mitochondria. Note the small granules (*gr*) in one profile. These are of unknown nature. Several patches of extracellular matrix material occur as in the insets. There also are suggestions of desmosomoid differentiations as in the upper left enlargement (arrow) from another micrograph of a similar region. Note the nucleus to the lower center having dense peripheral condensations of chromatin and scanty cytoplasm. This might be an oligodendrogliacyte. Formalin–OsO_4 (Millonig)-fixed; $KMnO_4$-stained. × 10,000. Right inset × 44,000; left inset, × 48,000.

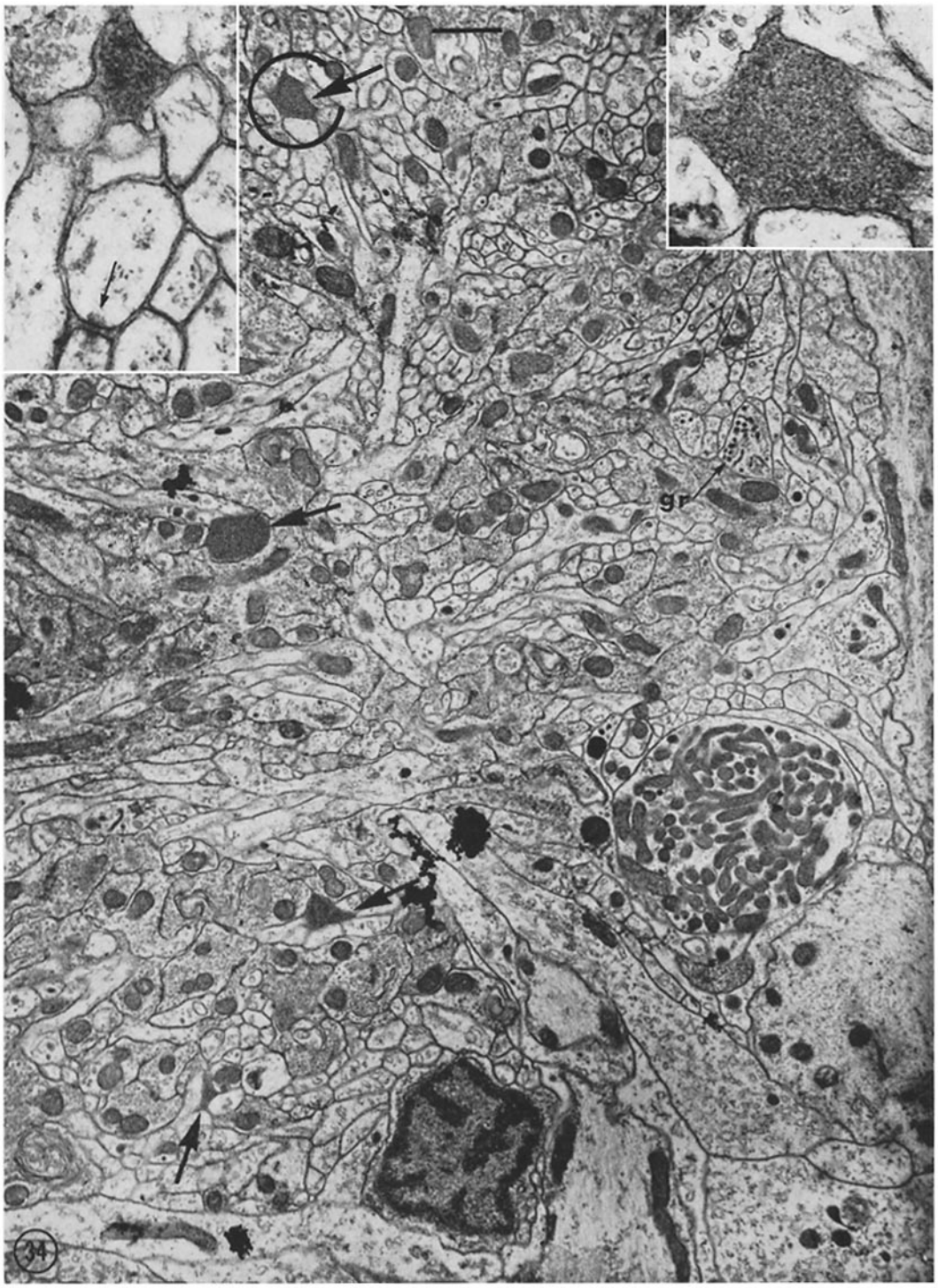
gr
34

Such elements are unusually sparse in brain and it seems reasonable to expect to find large numbers of desmosomes particularly in synaptic regions where things obviously need to be held together unusually well.

Along these same lines, we show in Fig. 22 and possibly in Fig. 10 (lower inset) a type of intimate membrane contact that raises the same questions with regard to our synaptic discs. We feel quite sure that in Fig. 22 the membranes of two adjacent glia cells are involved, since both cells contain characteristic glia filaments (50, 15). Their junctional complexes are like the ones previously described between glia cells in brain by Gray (51) and Peters (91). They are also similar to regions of close membrane contact with external compound membrane formation that have been observed by Robertson between intestinal epithelial cells (113), capillary endothelial cells (115), and in nodes of Ranvier (108, 111), and recently by Farquhar and Palade (33, 34) in intestinal and other glandular mucosae. In fact, nerve myelin is the extreme example of such a tight junction of membranes. A most reasonable functional role in all these situations has seemed to be the restriction of free diffusion of materials along the clefts between the cells involved. Are we then justified in assigning any unique role to the synaptic discs in synaptic transmission? The situation is directly analogous to that involving the desmosome-like regions and we are left in the same position of uncertainty.

The various differentiated structures discussed all occur in synapses, and it is reasonable to ascribe some role to each of them in the physiological processes of synaptic transmission. The main purpose of the above discussion is to interject a note of caution into the problem of deciding too soon precisely what role they may play. Their functions could be directly related to the functions of their counterparts elsewhere or they could be different. We have no way to decide with our present incomplete information.

Another problem is the involvement of various types of anatomical structures outside the immediate contacting membranes with the physiological events of synaptic transmission. The anatomical investigations of synapses have been much concerned with the physiological concept that a transmitter substance is responsible for activity in most central nervous system synapses. That acetylcholine is one of the most important transmitters and that it and other possible transmitters may be enclosed in packets in unit membrane bounded vesicles ~400 A in diameter, like the ones found accumulated in large numbers by Palade and Palay (83), Robertson (107, 112) and others (8) in vertebrate motor end plates, and by De Robertis and Bennett (26) and others in vertebrate and invertebrate synapses, has become a widely discussed concept although it remains unproven in rigorous terms. Such vesicular structures were called synaptic vesicles by De Robertis and Bennett (26). Del Castillo and Katz (21), from electrophysiological studies of the miniature end plate potentials of frog motor nerve endings provided early evidence suggesting that each vesicle in a motor end plate might contain a packet of acetylcholine molecules, giving a miniature potential on discharge by coalescence with the presynaptic membrane. Recent work by some groups has been concentrated on attempts to

FIGURE 35 Low power view of Mauthner axon with its cap neuropil. The axon is cut obliquely. Note the granules (*gr*) in the central profile. Formalin–OsO_4-fixed; $KMnO_4$-stained. × 7,000.

FIGURE 36 Higher magnification oblique section of Mauthner axon. Formalin–OsO_4-fixed; $KMnO_4$-stained. × 56,000.

FIGURE 37 Section of node in medulla. Note the tenuous remnants of extracellular matrix material (*) at the arrows. OsO_4-fixed; $KMnO_4$-stained. × 27,000.

FIGURE 38 Myelinated fiber with node in medulla near Mauthner cell. Note the multiple mesaxons perpendicular to the axon and the dense granules in the cytoplasm between separated myelin lamellae. The axon contains prominent neurofilaments and endoplasmic reticulum (*ER*) membranes. The nature of the area (*X*) bordered by the *ER* is undecided. Note the dense extracellular matrix material (*) bordering the unmyelinated axon surface. The photographic masking technique described by Gonzales (47) was used for this micrograph. Formalin–OsO_4-fixed; uranyl acetate-stained. × 27,000.

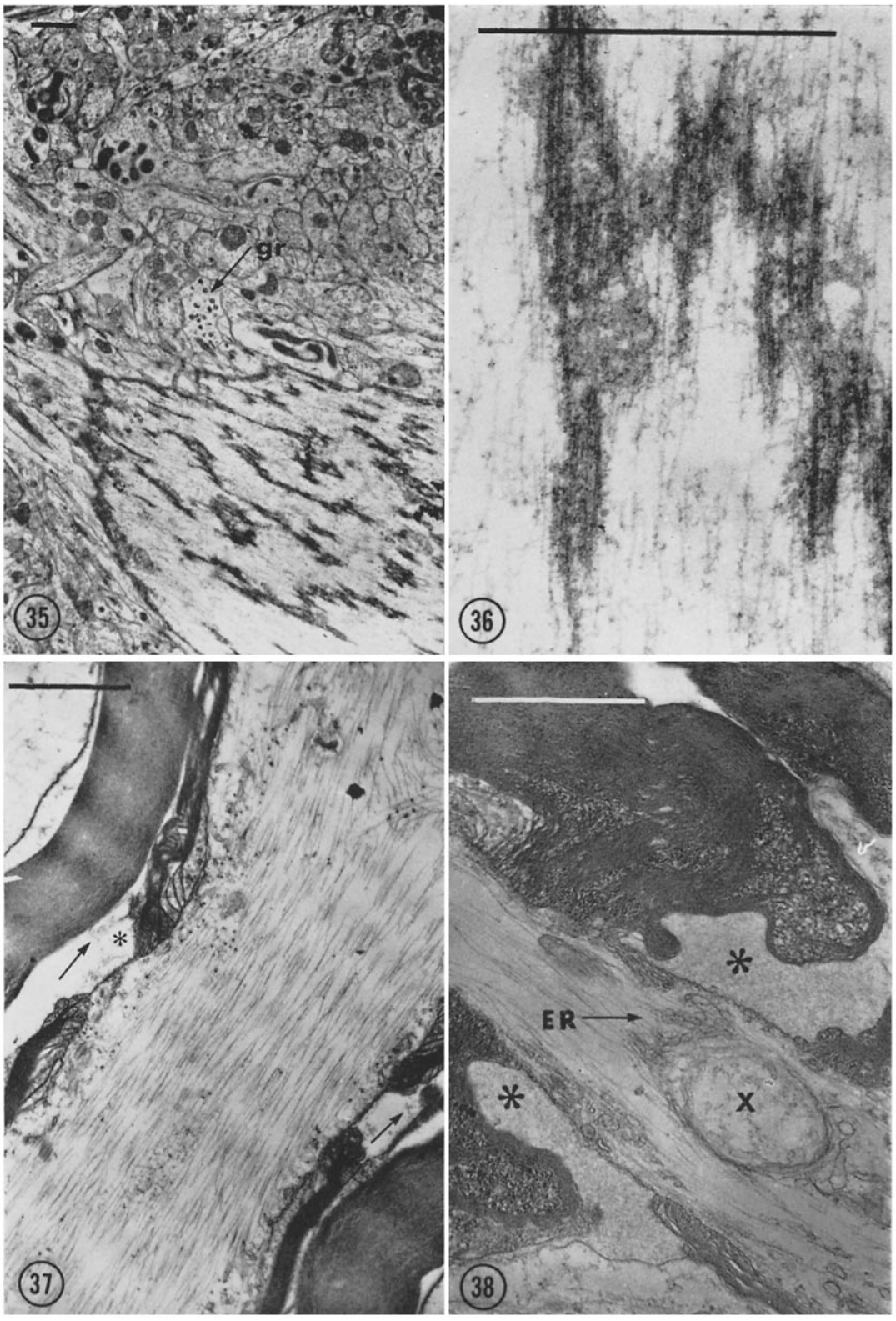
gr
35
36
37
38
ER
X

isolate synaptic vesicles and measure their content of acetylcholine and other possible transmitters. Some measure of success has been achieved in associating acetylcholine activity with synaptic vesicles by Gray and Whittaker (53, 54, 133) and by De Robertis *et al.* (27). In relation to this problem, Wolfe *et al.* (136) have recently shown an association between tritiated norepinephrine and vesicle-containing sympathetic nerve endings in rat pineal bodies. This supports the belief that such vesicles contain a neurohumoral agent.

That direct electrical synaptic transmission might be important in the central nervous system has been considered in the past (3), but work in recent years has led to the belief that chemical neurohumoral transmission dominates in vertebrate central nervous systems (see Eccles, reference 29). Recently Furshpan and Potter (41) have produced very convincing evidence of electrical synaptic transmission in crayfish giant fiber synapses. This has been correlated with the electron microscope demonstration of especially intimate pre- and postsynaptic unit membrane contact (external compound membranes) in these synapses by Robertson (114, 116, 117) (See also Hama, reference 55). Recently, experimental electrophysiological evidence of electrically mediated inhibitory effects in the region of the axon cap of Mauthner cells in goldfish has been reported by Furakawa and Furshpan (38, 40). Our findings in the cap region offer but little basis for correlation with this evidence, beyond perhaps our finding of relatively little over-all extracellular matrix material in this region. However, there does seem to be some possibility of a more direct correlation with physiological findings in the lateral dendrite synapses. Here, there is a clear morphological distinction between the club endings and the boutons terminaux. Synaptic vesicles are very prominent in the boutons and, following the prevailing concepts, may be considered to suggest neurohumoral transmission. The club endings, while containing moderate numbers of vesicles, differ distinctly from the boutons by showing closed intermembrane gaps, or synaptic discs. Because such intimate membrane contacts were like those we had associated with electrical transmission in crayfish ganglia, and because external compound membranes seem to occur at junctions between cardiac muscle cells (125) where electrical transmission is probable, we wondered about the possibility of electrical transmission in the club endings. It was gratifying to learn, while we were making our structural observations, that Furshpan (39) found electrophysiological evidence that suggests the possibility of excitatory electrical transmission at the eighth nerve endings on the Mauthner cell. It thus seems reasonable to say that the presence of external compound membranes in synapses should at least make one think of electrical transmission. If this is so, the function of the vesicles in club endings is enigmatic unless we suppose that these synapses may transmit both electrically and neurohumorally. Perhaps this idea of dual transmission mechanisms in one synapse should be explored further, but we must keep in mind the fact that both of the structural differentiations on which it is based are found elsewhere in locations suggesting other functions. We may conclude that other more subtle structural differentiations that may be peculiar to synaptic transmission should be sought. The paper that follows this one shows that such more refined differentiations do exist in the synaptic discs but we still do not know to what extent these may be uniquely involved in physiological synaptic transmission, because related structures in other tissues may be found to have the same features.

Mr. Bodenheimer and Mr. Stage are third year students at Harvard Medical School.

The authors wish to acknowledge their appreciation of the technical assistance in all phases of the work of Miss Janet Lamborghini and the photographic assistance of Mr. Alfred Ley. Mrs. Ann Doughty assisted with the histological work. We are indebted to Professor Jordi Folch-Pi for his constant support. The work was supported by Grant B-2665 from the Council of Neurological Diseases and Blindness of the National Institutes of Health.

Received for publication, March 19, 1963.

BIBLIOGRAPHY

1. ALLEN, J. N., Extracellular space in the central nervous system, *A.M.A. Arch. Neurol. and Psychiat.*, 1955, **73**, 241.
2. AMBERSON, W. R., NASH, T. P., MULDER, A. G., and BINNS, D., The relationship between tissue chloride and plasma chloride, *Am. J. Physiol.*, 1938, **122**, 224.
3. ARVANITAKI, A., Effects evoked in an axon by

the activity of a contiguous one, *J. Neurophysiol.*, 1942, **5**, 89.

4. BARLOW, C. F., DOMEK, N. S., GOLDBERG, M. A., and ROTH, L. J., Extracellular brain space measured by S^{35} sulfate, *Arch. Neurol.*, 1961, **5**, 102.
5. BARTELMEZ, G. W., Mauthner's cell and the nucleus motorius tegmenti, *J. Comp. Neurol.*, 1915, **25**, 87.
6. BARTELMEZ, G. W., and HOERR, N. L., The vestibular club endings in Ameiurus. Further evidence on the morphology of the synapse, *J. Comp. Neurol.*, 1933, **57**, 401.
7. BECCARI, N., Ricerche sulle cellule e fibre del Mauthner e sulle loro connessioni in pesci ed anfibii, *Arch. Ital. Anat. e Embryol.*, 1908, **6**, 660.
8. BIRKS, R., HUXLEY, H. E., and KATZ, B., The fine structure of the neuromuscular junction of the frog, *J. Physiol.*, 1960, **150**, 134.
9. BLACKSTAD, T. W., A note on the electron microscopy of the fascia dentata, *Acta Morphol. Neerl.-Scand.* 1961, **3**, 395.
10. BLACKSTAD, T. W. and DAHL, H. A., Quantitative evaluation of structures in contact with neuronal somata, *Acta Morphol. Neerl.-Scand.*, 1962, **4**, 329.
11. BODIAN, D., The structure of the vertebrate synapse. A study of the axon ending on Mauthner's cell and neighboring centers in the goldfish, *J. Comp. Neurol.*, 1937, **68**, 117.
12. BODIAN, D., Cytological aspects of synaptic function, *Physiol. Rev.*, 1942, **22**, 146.
13. BODIAN, D., Introductory survey of neurones, *Cold Spring Harbour Symp. Quant. Biol.*, 1952, **17**, 1.
14. BOYCOTT, B. B., GRAY, E. G., and GUILLERY, R. W., Synaptic structure and its alteration with environmental temperature: a study by light and electron microscopy of the central nervous system of lizards, *Proc. Roy. Soc. London Series B.*, 1961, **154**, 151.
15. BUNGE, M. B., BUNGE, R. P., and RIS, H., Ultrastructural study of remyelination in an experimental lesion in adult cat spinal cord, *J. Biophysic. and Biochem. Cytol.*, 1961, **10**, 67.
16. CAJAL, S. RAMÓN, Histologie du Systéme Nerveux de l'Homme et des Vertebres, (L. Azoulay, translator), 1952, Madrid, Instituto Ramon y Cajal, 1961, 2 vols.
17. COGHILL, G. E., New anatomical relations and probable function of Mauthner's fiber, *Psychiat. en Neurol. Bladen*, 1934, **38**, 386.
18. COLONNIER, M. and GRAY, E. A., Degeneration in the cerebral cortex, *in* 5th International Congress for Electron Microscopy, Philadelphia, 1962, (S. S. Breese, Jr., editor), New York, Academic Press, Inc., 1962, **2**, U-3.
19. DAVSON, H. and SPAZIANI, The blood-brain barrier and the extracellular space of brain, *J. Physiol.*, 1959, **149**, 135.
20. DE IRALDI, A., PELLEGRINO and DE ROBERTIS, E., Study of a special neurosecretory neuron in the nerve cord of the earthworm, 5th International Congress for Electron Microscopy, Philadelphia, 1962, (S. S. Breese, Jr., editor), New York, Academic Press, Inc., 1962, **1**, U-7.
21. DEL CASTILLO, J. and KATZ, B., Biophysical aspects of neuromuscular transmission, *Prog. Biophysic. and Biophysic. Chem.*, 1956, **6**, 121.
22. DE LORENZO, A. J., The fine structure of synapses in the ciliary ganglion of the chick, *J. Biophysic. and Biochem. Cytol.*, 1960, **7**, 31.
23. DE LORENZO, A. J., Electron microscopy of the cerebral cortex. I. Ultrastructure and histochemistry of synaptic junctions, *Bull. Johns Hopkins Hosp.*, 1961, **108**, 258.
24. DEMPSEY, E. W. and LUSE, S., Fine structure of the neuropil in relation to neuroglia cells *in* Biology of Neuroglia, (W. F. Windle, editor), Springfield, Illinois, Charles C. Thomas Co., 1958, 108–129.
25. DEMPSEY, E. W. and WISLOCKI, G. B., An electron microscopic study of the blood-brain barrier in the rat employing silver nitrate as a vital stain, *J. Biophysic. and Biochem. Cytol.*, 1955, **1**, 245.
26. DE ROBERTIS, E. D. P., and BENNETT, H. S., Some features of the submicroscopic morphology of synapses in frog and earth worm, *J. Biophysic. and Biochem. Cytol.*, 1955, **1**, 47.
27. DE ROBERTIS, E. D. P., DE IRALDI, A., PELLEGRINO, A., RODRIQUEZ, J., and GOMEZ, C. J., On the isolation of nerve endings and synaptic vesicles, *J. Biophysic. and Biochem. Cytol.*, 1961, **9**, 229.
28. DOBBING, J., The blood-brain barrier, *Physiol. Rev.*, 1961, **41**, 130.
29. ECCLES, J. C., The mechanism of synaptic transmission, *Ergebn. Physiologie*, 1961, **51**, 299.
30. ESTABLE, C., REISSIG, M. and DE ROBERTIS, E., The microscopic and submicroscopic structure of the synapses in the ventral ganglion of the acoustic nerve, *J. Appl. Physics*, 1953, **24**, 1421.
31. FARQUHAR, M. G., Neuroglial structure and relationships as seen with the electron microscope, *Anat. Rec.*, 1955, **121**, 291.
32. FARQUHAR, M. G., and HARTMANN, J. F., Neuroglial structure and relationships as revealed by electron microscopy, *J. Neuropath. and Exp. Neurol.*, 1957, **16**, 18.
33. FARQUHAR, M. G., and PALADE, G. E., Tight intercellular junctions, Program of the 1st Annual

Meeting of the American Society for Cell Biology, Chicago, 1961, 57.

34. FARQUHAR, M. G., and PALADE, G. E., Junctional Complexes in various epithelia, *J. Cell Biol.*, 1963, **17**, 375.
35. FERNÁNDEZ-MORÁN, H., Cell membrane ultrastructure: Low-temperature electron microscopy and x-ray diffraction studies of lipoprotein components in lamellar systems, *in* Ultrastructure and Metabolism of the Nervous System, (S. Korey, editor), *Research Pub., Assn. Research Nervous and Ment. Dis.*, 1962, **11**, 235.
36. FORSTER, R. P., and TAGGART, J. V., Use of isolated renal tubule for the examination of metabolic processes associated with active cellular transport, *J. Comp. and Cell. Physiol.*, 1950, **36**, 251.
37. FRANKENHAEUSER, B. and HODGKIN, A., The after effects of impulses in the giant nerve fibers of Loligo, *J. Physiol.*, 1956, **131**, 341.
38. FURAKAWA, T., and FURSHPAN, E. J., Two inhibitory mechanisms in the Mauthner neurons of goldfish, *J. Neurophysiol.*, 1963, **26**, 140.
39. FURSHPAN, E. J., personal communication.
40. FURSHPAN, E. J., and FURAKAWA, T., Intracellular and extracellular responses of the several regions of the Mauthner cell of the goldfish, *J. Neurophysiol.*, 1962, **25**, 732.
41. FURSHPAN, E. J., and POTTER, D. D., Transmission at the giant motor synapses of the crayfish, *J. Physiol.*, 1959, **145**, 289.
42. GASIC, G., and BADINEZ, personal communication.
43. GASIC, G., and GASIC, T., Removal of Sialic acid from the cell coat in tumor cells and vascular endothelium and its effects on metastasis, *Proc. Nat. Acad. Sc.*, 1962, **48**, 1172.
44. GERSCHENFELD, H. M., Submicroscopic bases of synaptic organization in gastropod nervous systems, *in* 5th International Congress for Electron Microscopy, Philadelphia, 1962, (S. S. Breese, Jr., editor), New York Academic Press, Inc., 1962, **2**, U5.
45. GERSCHENFELD, H. M., WALD, F., ZADUNAISKY, J. A., and DE ROBERTIS, E. D. P., Function of astroglia in the water-ion metabolism of the central nervous system, *Neurology*, 1959, **9**, 412.
46. GLAUERT, A. M., ROGERS, G. E., and GLAUERT, R. H., Araldite as an embedding medium for electron microscopy, *J. Biophysic. and Biochem. Cytol.*, 1958, **4**, 191.
47. GONZALES, F., A masking technique for contrast control in electron micrographs, *J. Cell Biol.*, 1962, **15**, 146.
48. GRAY, E. G., Electron microscopy of dendrites and axons of the cerebral cortex, *J. Physiol.*, 1959, **145**, 25.
49. GRAY, E. G., Axo-somatic and axo-dendritic synapses of the cerebral cortex: an electron microscope study, *J. Anat.*, 1959, **93**, 420.
50. GRAY, E. G., Electron microscopy of neuroglial fibrils of the cerebral cortex, *J. Biophysic. and Biochem. Cytol.*, 1959, **6**, 121.
51. GRAY, E. G., Ultrastructure of synapses of the cerebral cortex and of certain specializations of neuroglial membranes, *in* Electron Microscopy in Anatomy, (J. D. Boyd, F. R. Johnson, and J. D. Lever, editors), London, Edward Arnold and Co., 1961, **54**, 54–73.
52. GRAY, E. G., The granule cells, mossy synapses and purkinje spine synapses of the cerebellum: light and electron microscope observations, *J. Anat.*, 1961, **95**, 345.
53. GRAY, E. G. and WHITTAKER, V. P., The isolation of synaptic vesicles from the central nervous system, *J. Physiol.*, 1960, **153**, 35.
54. GRAY, E. G., and WHITTAKER, V. P., The isolation of nerve endings from brain: an electron-microscopic study of cell fragments derived by homogenization and centrifugation, *J. Anat.*, 1962, **96**, 79.
55. HAMA, K., Some observations on the fine structure of the giant fibers of the crayfish (Cambarus virilus and Cambarus clarkii) with special reference to the submicroscopic organization of the synapse, *Anat. Rec.*, 1961, **141**, 275.
56. HAMLYN, L. H., The fine structure of the mossy fiber endings in the hippocampus of the rabbit, *J. Anat.*, 1962, **96**, 112.
57. HESS, A., The ground substance of the central nervous system revealed by histochemical staining, *J. Comp. Neurol.*, 1953, **98**, 69.
58. HORSTMANN, E., Die Structur der molekularen Schichten im Gehirn der Wirbettiere, *Naturwissenschaften*, 1957, **44**, 448.
59. HORSTMANN, E. and MEVES, H., Die Feinstructure des molekularen Rindengraues und ihre physiologische Bedeutung, *Z. Zellforsch, u. Micr. Anat.*, 1959, **49**, 569.
60. JONES, R. McC., McClung's Handbook of Microscopical Technique, New York, Paul B. Hoeber, Inc., 1950.
61. KANE, R. E., The mitotic apparatus, fine structure of the isolated unit, *J. Cell Biol.*, 1962, **15**, 279.
62. KARRER, H. E., The striated musculature of blood vessels, *J. Biophysic. and Biochem. Cytol.*, 1960, **8**, 135.
63. KLATZO, I., PIRAUX, A. and LASKOWSKI, E. S., The relationship between edema, blood-brain barrier and tissue elements in a local brain in-

jury, *J. Neuropath. and Exp. Neurol.*, 1958, **17**, 548.

64. LADMAN, A. J., The fine structure of the rod-bipolar cell synapse in the retina of the albino rat, *J. Biophysic. and Biochem. Cytol.*, 1958, **4**, 459.
65. LAJTHA, A., The development of the blood brain barrier, *J. Neurochem.*, 1960, **1**, 216.
66. LAWN, A. M., The use of potassium permanganate as an eleectron-dense stain for sections of tissue embedded in epoxy resin, *J. Biophysic. and Biochem. Cytol.*, 1960, **7**, 197.
67. LILLIE, R. D., *Histopathologic Technique*, New York, Blakiston Division, McGraw-Hill Book Company, Inc., 1948.
68. LUSE, S. A., Electron microscopy of the spinal cord, *Anat. Rec.*, 1955, **121**, 333.
69. LUSE, S. A., Electron microscopic observations of the central nervous system, *J. Biophysic. and Biochem. Cytol.*, 1956, **2**, 531.
70. LUSE, S. A., Histochemical implications of electron microscopy of the central nervous system, *J. Histochem. and Cytochem.*, 1960, **8**, 398.
71. LUSE, S. A. and HARRIS, B., Electronmicroscopy of the brain in experimental edema, *J. Neurosurg.*, 1960, **17**, 439.
72. MALM, M., *p*-toluenesulphonic acid as a fixative, *Quart. J. Micr. Sc.*, 1962, **103**, 163.
73. MANERY, J. F., Inorganic metabolism of the brain, *in* The Biology of Mental Health and Disease, Proceedings of the 27th Annual Conference of the Millbank Memorial Fund, New York, Paul B. Hoeber, Inc., 1952, 124–134.
74. MANERY, J. F., and HASTINGS, A. B., The distribution of electrolytes in mammalian tissues, *J. Biol. Chem.*, 1939, **127**, 657.
75. MANERY, J. F., and HAEGE, L. F., The extent to which radioactive chloride penetrates tissues and its significance, *Am. J. Physiol.*, 1941, **134**, 83.
76. MATURANA, H., The fine structure of the optic nerve of anurans: An electron microscope study, *J. Biophysic. and Biochem. Cytol.*, 1960, **7**, 107.
77. MAUTHNER, L., Untersuchungen über den Bau des Rückermantes der Fische, *Sitzungsber. k. Akad. Wissensch., Math.-naturwissench. Cl., Wien*, 1859, **34**, 31.
78. MAYNARD, E. A., and PEASE,, D. C., Electron microscopy of the cerebral cortex of the rat, *Anat. Rec.*, 1955, **121**, 440.
79. MAYNARD, E. A., SCHULTZ, R. L. and PEASE, D. C., Electron microscopy of the vascular bed of rat cerebral cortex, *Am. J. Anat.*, 1957, **100**, 409.
80. MCGEE-RUSSELL, S. M., and PALAY, S., personal communication.
81. METUZALS, J., Ultrastructure of Ranvier's node in central fibers, analyzed in serial sections, Electron microscopy, *in* 5th International Congress for Electron Microscopy, (S. S. Breese, Jr., editor), New York, Academic Press, Inc., 1962, **2**, N-9.
82. MILLONIG, G., Advantages of a phosphate buffer for OsO_4 solutions in fixation, *J. Appl.* Physics, 1961, **32**, 1637.
83. PALADE, G. E. and PALAY, S. L., Electron microscope observations of interneural and neuromuscular synapses, *Anat. Rec.*, 1954, **118**, 335
84. PALAY, S. L., Synapses in the central nervous system, *J. Biophysic. and Biochem. Cytol.*, 1956, **2**, 193.
85. PALAY, S. S., The morphology of synapses in the central nervous system, *Exp. Cell Research Suppl. 5*, 1958, 275.
86. PALAY, S. L., MCGEE-RUSSELL, S. M., GORDON, S. JR., and GRILLO, M. A., Fixation of neural tissues for electron microscope by perfusion with solutions of osmium tetroxide, *J. Cell Biol.*, 1962, **12**, 385.
87. PALAY, S. L. and PALADE, G. E., The fine structure of neurones, *J. Biophysic. and Biochem., Cytol.*, 1955, **1**, 68.
88. PEASE, D. C., Buffered formaldehyde as a killing agent and primary fixative for electron microscopy, *Anat. Rec.*, 1962, **142**, 342.
89. PETERS, A., The structure of myelin sheaths in the central nervous system of *Xenopus laevis* (Daudin), *J. Biophysic. and Biochem. Cytol.*, 1960, **7**, 121.
90. PETERS, A., The formation and structure of myelin sheaths in the central nervous system, *J. Biophysic. and Biochem. Cytol.*, 1960, **8**, 431.
91. PETERS, A., Plasma membrane contacts in the central nervous system, *J. Anat.*, 1962, **96**, 237.
92. PIAT, J., Further studies on the differentiation and growth of Mauthner's cell in Amblystoma, *J. Exp. Zool.*, 1950, **113**, 379.
93. REED, D. J., and WOODBURY, D. M., I^{131} distribution in cerebral cortex, cerebrospinal fluid, and plasma of rats, *Pharmacologist*, 1960, **2**, pt. 2, 92.
94. RETZLAFF, E., A mechanism for excitation and inhibition of the Mauthner's cells in Teleost: A histological and neurophysiological study, *J. Comp. Neurol.*, 1957, **107**, 209.
95. RETZLAFF, E., Neurohistological basis for the functioning of paired half-centers, *J. Comp. Neurol.*, 1954, **101**, 407.
96. REVEL, J. P., Napolitano, L., and FAWCETT, D. W., Identification of glycogen in electron

micrographs of thin tissue sections, *J. Biophysic. and Biochem. Cytol.*, 1960, **8**, 575.

97. RICHARDSON, K. C., Formalin-osmium tetroxide fixation of nuclei, tracts or discrete regions of the central nervous system for electron microscopy, *Anat. Rec.*, 1961, **139**, 333.
98. RITCHIE, J. M., and STRAUB, R. W., The hyperpolarization which follows activity in mammalian non-medullated fibers, *J. Physiol.*, 1957, **136**, 80.
99. ROBERTSON, J. D., Ultrastructure of an invertebrate synapse, Ph.D. Thesis, Massachusetts Institute of Technology Library, 1952.
100. ROBERTSON, J. D., Addendum to Neurons of Arthropods, *Cold Spring Harbor Symp. Quant. Biol.*, 1952, **17**, 161.
101. ROBERTSON, J. D., Ultrastructure of two invertebrate synapses, *Proc. Soc. Exp. Biol. and Med.*, 1953, **82**, 219.
102. ROBERTSON, J. D., The ultrastructure of two invertebrate synapses, *J. Appl. Physics*, 1953, **24**, 117.
103. ROBERTSON, J. D., Electron microscope studies of an invertebrate synapse, *Fed. Proc.*, 1954, **13**, 119.
104. ROBERTSON, J. D., Recent electron microscope observations on the ultrastructure of the crayfish median-to-motor giant synapse, *Exp. Cell Research*, 1955, **8**, 226.
105. ROBERTSON, J. D., The ultrastructure of the myelin sheath near nodes of Ranvier, *J. Physiol.*, 1956, **135**, 56.
106. ROBERTSON, J. D., The ultrastructure of nodes of Ranvier in frog nerve fibers, *J. Physiol.*, 1957, **137**, 8.
107. ROBERTSON, J. D., The ultrastructure of a reptilian myoneural junction, *J. Biophysic. and Biochem. Cytol.*, 1956, **2**, 381.
108. ROBERTSON, J. D., New observations on the ultrastructure of the membranes of frog peripheral nerve fibers, *J. Biophysic. and Biochem. Cytol.*, 1957, **3**, 1043.
109. ROBERTSON, J. D., Structural alterations in nerve fibers produced by hypotonic and hypertonic solutions, *J. Biophysic. and Biochem. Cytol.*, 1958, **4**, 349.
110. ROBERTSON, J. D., The ultrastructure of cell membranes and their derivatives, *Biochem. Soc. Symp.*, 1959, **16**, 3.
111. ROBERTSON, J. D., Preliminary observations on the ultrastructure of nodes of Ranvier, *Z. Zellforsh. u. Mikr. Anat.*, 1959, **50**, 553.
112. ROBERTSON, J. D., Electron microscopy of the motor end plate and the neuromuscular spindle, *Am. J. Phys. Med.*, 1960, **39**, 1.
113. ROBERTSON, J. D., The molecular structure and contact relationships of cell membranes, *in* Progress in Biophysics, (B. Katz and J. A. V. Butler, editors), Pergamon Press, 1960, 343.
114. ROBERTSON, J. D., Ultrastructure of excitable membranes and the crayfish median giant synapse, *Ann. New York Acad. Sc.*, 1961, **94**, 339.
115. ROBERTSON, J. D., The unit membrane, *in* Electron Microscopy in Anatomy, (J. D. Boyd, F. R. Johnson, and J. D. Lever, editors), London, Edward Arnold and Co., 1961, 74–79.
116. ROBERTSON, J. D., Unit membrane contact relationships in myelin and synapses, in *Anat. Rec.*, 1962, **142**, 273.
117. ROBERTSON, J. D., Factors influencing the width of the gap between paired unit membranes in dissociated and reconstituted myelin with related observations of unusual gap widths in synapses, in *Anat. Rec.*, 1962, **142**, 343.
118. ROBERTSON, J. D., The occurrence of a subunit pattern in the unit membranes of club endings in Mauthner cell synapses in goldfish brains, *J. Cell Biol.*, 1963, **9**, 201.
119. ROBERTSON, J. D., BODENHEIMER, T. S. and STAGE, D. E., An electron microscope study of the Mauthner cell, Program of the 2nd Annual Meeting of the Society for Cell Biology, San Francisco, California, 1962, 194.
120. ROSENBLUTH, J., Subsurface cisterns and their relationship to the neuronal plasma membrane, *J. Cell Biol.*, 1962, **13**, 405.
121. RUTHMAN, A., The fine structure of the meiotic spindle of the crayfish, *J. Biophysic. and Biochem. Cytol.*, 1959, **5**, 177.
122. SATIR, P. G. and PEACHEY, L. D., Thin sections II. A simple method for reducing compression artifacts, *J. Biophysic. and Biochem. Cytol.*, 1958, **4**, 345.
123. SCHULTZ, R., MAYNARD, E. A., and PEASE, D. C., Electron microscopy of neurons and neuroglia of cerebral cortex and corpus callosum, *Am. J. Anat.*, 1957, **100**, 369.
124. SJÖSTRAND, F. S., Ultrastructure of retinal rod synapses of the guinea pig eye as revealed by three-dimensional reconstructions from serial sections, *J. Ultrastruct. Research*, 1958, **2**, 122.
125. SJÖSTRAND, F. S., ANDERSSON-CEDERGREN, E., and DEWEY, M. M., The ultrastructure of the intercalated discs of frog, mouse and guinea pig cardiac muscle, *J. Ultrastruct., Research*, 1958, **1**, 271.
126. STEFANELLI, A., The Mauthnerial apparatus in the Ichthyopsida; its nature and function and correlated problems of neurohistogenesis, *Quart. Rev. Biol.*, 1951, **26**, 17.
127. STREICHER, E., and PRESS, G. D., The thio-

cyanate space of rat brain, *Am. J. Physiol.*, 1961, **201**, pt. 2, 334.

128. UZMAN, B. G. and NOGUEIRA-GRAF, G., Electron microscope studies of nodes of Ranvier in mouse sciatic nerves, *J. Biophysic. and Biochem. Cytol.*, 1957, **3**, 589.
129. UZMAN, B. G. and VILLEGAS, G. M., A comparison of nodes of Ranvier in sciatic nerves with node-like structures in optic nerves of the mouse, *J. Biophysic. and Biochem. Cytol.*, 1960, **7**, 761.
130. VAN HARREVELD, A., Changes in volume of cortical neuronal elements during asphyxiation, *Am. J. Physiol.*, 1957, **191**, 233.
131. VAN HARREVELD, A., and SCHADÉ, J. P., On the distribution and movements of water and electrolytes in the cerebral cortex, *in* Structure and Function of the Cerebral Cortex, Proc. Second International Meeting of Neurobiologists, Amsterdam, 1959, (D. B. Towes and J. P. Schadé, editors), Amsterdam, Elsevier Publishing Company, 1960, 239–256.
132. WATSON, M. L., Staining of tissue sections for electron microscopy with heavy metals, *J. Biophysic. and Biochem. Cytol.*, 1958, **4**, 475.
133. WHITTAKER, V. P. and GRAY, E. G., The synapse: biology and morphology, *Brit. Med. J.*, 1962, **18**, 223.
134. WILSON, D. M., Function of giant Mauthner's neurons in the lungfish, *Science*, 1959, **129**, 841.
135. WOLFE, D. E., Electron microscopic criteria for distinguishing dendrites from preterminal nonmyelinated axons in the area postrema of the rat, and characterization of a novel synapse, 1st Annual Meeting of the American Society for Cell Biology, Chicago, 1961, 288.
136. WOLFE, D. E., POTTER, L. T., RICHARDSON, K. C., and AXELROD, J., Localizing tritiated norepinephrine in sympathetic axons by electron microscopic autoradiography, *Science*, 1962, **138**, 440.
137. WOODBURY, D. M., *in* Fine structure of the neuropil in relation to neuroglia cells, *in* The Biology of Neuroglia, (W. F. Windle, editor), Springfield, Illinois, Charles C. Thomas, Co., 1958, 120–127.
138. WOODBURY, D. M., TIMANAS, P. S., KOCH, A., and BALLARD, A., Distribution of radiochloride, radiosulfate and inulin in brain of rats, *Fed. Proc.*, 1956, **15**, 501.
139. WYCKOFF, R. W. G., and YOUNG, J. Z., The nerve cell surface, *J. Anat.*, 1954, **88**, 568.
140. WYCKOFF, R. W. G., and YOUNG, J. Z., The motor-neuron surface, *Proc. Roy. Soc. London, Series B.*, 1956, **144**, 440.